KONINKLIJK NEDERLANDS METEOROLOGISCH INSTITUUT

WETENSCHAPPELIJK RAPPORT

SCIENTIFIC REPORT

W.R. 83 - 4

A.A.M. Holtslag en A.P. van Ulden

De meteorologische aspecten van luchtverontreinigingsmodellen: eindrapport van het project klimatologie verspreidingsmodellen

De Bilt, 1983

Publikatienummer: K.N.M.I. W.R. 83-4 (FM)

Koninklijk Nederlands Meteorologisch Instituut
Fysisch Meteorologisch Onderzoek
Postbus 201
3730 AE De Bilt
Nederland

U.D.C.: 551.510.42 :
551.511.6 :
551.510.522:
551.551.8

De meteorologische aspecten van luchtverontreinigingsmodellen

Eindrapport van het project
klimatologie verspreidingsmodellen.

A.A.M. Holtslag
A.P. van Ulden

K.N.M.I., De Bilt
Januari 1983

Dit onderzoek werd verricht op verzoek van het Ministerie van Volkshuisvesting, Ruimtelijke Ordening en Milieubeheer (Direktie Lucht).

Inhoudsopgave

Hoofdstuk III

Simple estimates of nighttime surface fluxes from routine weather data (referentie [6] van hoofdstuk I).

Samenvatting

In dit rapport worden de resultaten van het project "klimatologie verspreidingsmodellen" gepresenteerd. Dit project werd in 1979 op het KNMI gestart en ten dele gefinancierd door het toenmalige Ministerie van Volksgezondheid en Milieuhygiëne. De bedoeling van het project was het verkrijgen van een nieuwe klassificatie van de atmosferische stabiliteit nabij het aardoppervlak. Deze stabiliteit bepaalt de mate waarin vertikale bewegingen worden versterkt of verzwakt door de aanwezigheid van turbulentie. Daarnaast zijn voor de verspreiding van luchtverontreiniging de transportsnelheid en de dikte van de grenslaag van belang. Deze meteorologische aspecten worden in hoofdstuk I van dit rapport kwalitatief besproken. Ook wordt in dit hoofdstuk ingegaan op de huidige berekenings-methode voor de verspreiding van luchtverontreiniging. Daarnaast wordt een aanzet gegeven voor een verbeterde berekeningsmethode. De verbeterde methode maakt gebruik van de in dit onderzoek ontwikkelde stabiliteitsclassificatie. Deze stabiliteitsclassificatie omvat de praktische bepaling van de zogenaamde wrijvingssnelheid en de voelbare warmtestroom. Hiervoor worden routinematig beschikbare meteorologische gegevens gebruikt. In paragraaf 5 van hoofdstuk I wordt een samenvatting gegeven van de ontwikkelde methodiek. Ook worden hier de toepassingen van de methodiek besproken voor de verspreiding van luchtverontreiniging. In de hoofdstukken II en III van dit rapport wordt voor respectievelijk de dag en de nacht ingegaan op de wetenschappelijke achtergronden van de ontwikkelde methodiek. Daarbij worden de resultaten van de methodiek vergeleken met waarnemingen aan de meteorologische mast te Cabauw. Uit deze vergelijking volgt een goede overeenkomst. Met de ontwikkelde methodiek kunnen fysische processen in de atmosferische grenslaag beter worden beschreven. Daardoor kan in principe ook de verspreiding van luchtverontreini-ging beter worden beschreven.

Hoofdstuk I. De berekening van de verspreiding van luchtverontreiniging.*

1. Inleiding.

Voor de berekening van de verspreiding van luchtverontreiniging is het zinvol om drie groepen van processen te onderscheiden. De eerste groep volgt uit de karakteristieken van de bron. Deze bepalen op welke manier de verontreiniging in de atmosfeer komt. De tweede groep wordt bepaald door de toestand van de atmosfeer en de eigenschappen van het terrein. De derde groep wordt gevormd door de verwijderingsmechanismen zoals chemische reaktie en depositie aan het aardoppervlak. De laatste groep komt hier verder niet aan de orde.

Voor de eerste groep van processen kunnen we een onderscheid maken tussen vrijstaande bronnen en beschutte bronnen. Een bron kan als vrijstaand worden beschouwd wanneer de bron hoger is dan 3 maal de hoogte van obstakels in de omgeving. Dan wordt de verspreiding niet direkt beïnvloed door de luchtstromingen rond de obstakels. Wel wordt de verspreiding beïnvloed door de uittreesnelheid en de temperatuur van de lozing welke resulteren in pluimstijging [10]. Voor vrijstaande relatief hoge bronnen kan de dispersie in principe worden berekend. Dit geldt ook voor relatief lage en beschutte bronnen op grotere afstand. Dan worden de bronnen in groepen samen genomen tot een oppervlaktebron of een lijnbron (zoals bij verkeersemissies en lekkages bij industriecomplexen). Voor kortere afstanden moeten windtunnelproeven gedaan worden om de verspreiding te beschrijven.

Ook vloeistoflozingen kunnen aanleiding geven tot luchtverontreiniging. De manier waarop hangt samen met de kooktemperatuur van de geloosde stof en de temperatuur en druk van de stof ten tijde van de emissie. Van groot belang is de dichtheid van het gasmengsel dat na het vrijkomen ontstaat. Bij mengsels met een hoge dichtheid (zogenaamde "zware gassen") volgt uitstroming over het aardoppervlak onder invloed van de zwaartekracht [19, 22].

In dit rapport wordt nader ingegaan op de meteorologische aspecten bij de berekening van de verspreiding van luchtverontreiniging. Deze meteorologishe aspecten worden behandeld in paragraaf 2. In de paragrafen 3 en 4 worden respectievelijk bestaande en verbeterde berekeningswijzen voor de verspreiding behandeld. Tot slot wordt in paragraaf 5 een samenvatting gegeven van een

*Dit hoofdstuk is ten dele gebaseerd op referentie [23].

methodiek voor de praktische bepaling van twee belangrijke meteorologische parameters, die een rol spelen bij de verspreiding van luchtverontreiniging. In de hoofdstukken II en III wordt gedetailleerd ingegaan op de bepaling van deze parameters.

2. De meteorologische aspecten.

De verspreiding van verontreiniging in de atmosfeer geschiedt vrijwel uitsluitend door luchtbewegingen. Moleculaire diffusie kan hierbij worden verwaarloosd. Luchtbewegingen variëren sterk in ruimte en tijd. Veelal wordt een indeling gemaakt naar de fluctuatieduur. Fluctuaties die korter duren dan circa een half uur worden turbulentie genoemd. De luchtbeweging gemideld over een half uur wordt de wind genoemd. De wind zelf varieert ook weer met de plaats en tijd. De wind zorgt in de eerste plaats voor het horizontale transport van de verontreiniging. Tijdens dit transport vindt tevens dispersie plaats: de pluim wordt wijder zowel dwars op de wind als verticaal. Tot afstanden van zo'n 10 km wordt de dispersie vooral bepaald door de turbulentie-intensiteit. Op grotere afstand gaan ook de variaties van de wind in ruimte en tijd een belangrijke rol spelen.

In het algemeen wordt de turbulentie-intensiteit bepaald door de windsnelheid, de ruwheid van de bodem en de stabiliteit van de atmosfeer. De betekenis van deze grootheden en hun samenhang met de grenslaag wordt in het volgende uitgewerkt.

2.1. De wind.

Het verschijnsel wind is een gevolg van het bestaan van horizontale verschillen in luchtdruk. Lucht stroomt van hoge naar lage druk. Door de draaiing van de aarde is er ook een Coriolis-kracht, die maakt dat de luchtbeweging (op het noordelijk halfrond) naar rechts wordt afgebogen (Wet van Buys Ballot [10]). Hoog in de atmosfeer is het effect van de Corioliskracht zodanig dat daar de wind evenwijdig waait met lijnen van gelijke druk (isobaren). Hier waait de vrije wind, ook wel geowind G genoemd. Dichterbij het aardoppervlak - in de atmosferische grenslaag - speelt ook de wrijving met het aardoppervlak een rol. Tengevolge van wrijving is de windsnelheid in de grenslaag in het algemeen kleiner dan de geowind, terwijl ook de windrichting afwijkt. In de praktijk is de

wind in de grenslaag tegen de klok ingedraaid ten opzichte van de geowind. De draaiingshoek kan 0 tot 45 graden bedragen.

Ook binnen de grenslaag variëren windsnelheid en windrichting nog met de hoogte. Het meest duidelijk is de snelle toename met de hoogte van de windsnelheid dichtbij het aardoppervlak. In veel gevallen is de windsnelheid evenredig met de logarithme van de hoogte:

$$U_z = (u_*/k) \ln (z/z_o) . \qquad (1)$$

Hier is U_z de windsnelheid, z de hoogte, u_* de wrijvingssnelheid, k = 0.40 de Von Kármán constante en z_o de ruwheidslengte. De ruwheidslengte wordt bepaald door de terreingesteldheid. Voor open grasland is $z_o \simeq 0.03$ m, voor cultuurland met obstakels is $z_o \simeq 0.25$ m en voor woongebieden en bossen is $z_o \simeq 1$ m [25].

In (1) bepaalt z_o de verhouding tussen U_z en u_* voor gegeven hoogte z. Boven ruw terrein is u_* relatief groot, boven glad terrein relatief klein. De wrijvingssnelheid u_* is dus een maat voor de turbulentie die nabij het aardoppervlak wordt opgewekt door wrijving. Deze turbulentie wordt mechanische turbulentie genoemd. Het logarithmisch wind profiel (1) geldt alleen in een neutraal gelaagde atmosfeer. De atmosfeer wordt neutraal genoemd wanneer vertikale bewegingen noch worden versterkt noch worden verzwakt. Wanneer dit niet het geval is moeten op (1) stabiliteitscorrecties worden uitgevoerd. De invloed van de stabiliteit komt in paragraaf 2.2. aan de orde.

2.2. De stabiliteit van de atmosfeer nabij het aardoppervlak.

Voor het beschrijven van de stabiliteit van de atmosfeer maken we onderscheid tussen de dag en de nacht. Overdag wordt door de zon het aardoppervlak en daardoor de lucht direkt erboven verwarmd. De lucht wordt echter zelf nauwelijks direkt verwarmd door de zonnestraling. Dit leidt tot een onstabiele gelaagdheid in de atmosfeer: De warme lucht van beneden stijgt op en wordt vervangen door koudere lucht van boven. Bij dit proces is er dus een netto warmtetransport naar boven. Hoe feller de zon schijnt des te sterker is dit proces en des te groter is de opwaartse warmtestroom en de productie van convectieve turbulentie die hiermee gepaard gaat. Daardoor is de grootte van de opwaartse warmtestroom een

goede maat voor de mate van onstabiliteit en de opgewekte turbulentie. Bij een hoge zonnestand en weinig bewolking is de warmtestroom en de sterkte van de turbulentie relatief groot. Bij lage zonnestand en/of grote bewolkingsgraad is de warmtestroom klein en de turbulentie relatief zwak.

We hebben dus nu twee processen die de sterkte van de turbulentie bepalen. De eerste is de wrijving, die gekarakteriseerd wordt door de wrijvingssnelheid u_* en die wordt bepaald door de windsnelheid en de ruwheid van het terrein. De tweede is de warmtestroom die voornamelijk wordt bepaald door de zonshoogte en de bewolkingsgraad. Als er een positieve opwaartse warmtestroom is zal de turbulentie dus sterker zijn dan in een neutrale atmosfeer, waarin de warmtestroom nul is. In hoofdzaak wordt de turbulentiesterkte overdag dus bepaald door de windsnelheid, de ruwheid, de zonshoogte en de bewolking. Op dit principe zijn de bekende Pasquill stabiliteitsklassen gebaseerd, zij het dat het effect van de ruwheid niet expliciet is meegenomen [10].

's Nachts is de situatie wat anders. Dan koelt het aardoppervlak af door uitstraling. Door mechanische turbulentie wordt lucht in aanraking gebracht met het aardoppervlak. Daardoor zal ook de lucht afkoelen en wel van onder af aan. Het gevolg is dat 's nachts onderin koude lucht aanwezig is terwijl bovenin de lucht nog relatief warm is. Door turbulentie wordt de warme lucht naar beneden getransporteerd, hetgeen resulteerd in een (negatieve) neerwaartse warmtestroom. Aangezien koude lucht het liefst beneden blijft is er sprake van een stabiele gelaagdheid. Deze stabiele gelaagdheid onderdrukt op haar beurt de turbulentie. In een stabiele atmosfeer is de turbulentie zwakker dan in een neutrale atmosfeer. Dit effect is des te sterker naarmate de negatieve warmtestroom sterker is. De warmtestroom hangt samen met de bewolkingsgraad. Naarmate er minder bewolking is, gaat de afkoeling van het aardoppervlak sneller en is de warmtestroom meer negatief. 's Nachts is de atmosfeer dus stabieler naarmate er minder bewolking is. De turbulentiesterkte 's nachts wordt nu bepaald door de windsnelheid, de ruwheid van het terrein en de bewolking ofwel door de wrijvingssnelheid u_* en de warmtestroom H.

We zien dat zowel overdag als 's nachts de turbulentiesterkte wordt bepaald door u_* en H. Aangezien dispersie direct samenhangt met de turbulentiesterkte is het te verwachten dat dispersie in termen van u_* en

H kan worden beschreven.

2.3. De grenslaag.

De atmosferische grenslaag is de onderste laag van de atmosfeer, die direkt door het aardoppervlak wordt beïnvloed. Het is de laag waarin duidelijke turbulentie-menging optreedt. Daarom wordt de grenslaag ook wel menglaag genoemd. Binnen deze laag wordt luchtverontreiniging redelijk snel (d.w.z. binnen een uur) vrijwel geheel gemengd. Boven de grenslaag vindt maar weinig dispersie plaats. Dit betekent dat de grenslaagdikte van groot belang is voor de verspreiding van luchtverontreiniging over grotere afstanden. De bovenkant van de grenslaag wordt gevormd door een stabiele laag waar door gebrek aan turbulentie de verontreinigingen niet ver in doordringen. Vaak is de stabiele laag een (temperatuur) inversie. In een inversie neemt de temperatuur met de hoogte toe. Zo'n laag is zeer stabiel omdat warmere lucht zich boven koudere bevindt.

Overdag is de grenslaag zelf onstabiel en alleen de top stabiel. Menging treedt op door het gecombineerd effect van wrijvingsturbulentie en warmteconvectie. 's Nachts is de gehele grenslaag min of meer stabiel. Menging treedt op door wrijvingsturbulentie, die door de stabiliteit wordt gedempt. Overdag verloopt de dispersie dus sneller dan 's nachts. Anderzijds is de grenslaagdikte overdag gewoonlijk veel groter dan 's nachts, vooral in de zomer. 's Nachts is de dikte van de orde 100 m. Overdag kan de maximum menghoogte variëren van zo'n 200 m in de winter tot zo'n 2000 m in de zomer.

3. De huidige berekeningsmethode voor de verspreiding van luchtverontreiniging met haar nadelen.

De thans veel gebruikte methodiek voor de berekening van de verspreiding van luchtverontreiniging is gebaseerd op het Gaussische pluimmodel [9,10]. Doorgaans wordt de vertikale dispersiecoëfficiënt van het Gaussische pluimmodel voor lage bronnen geschat uit de stabiliteitsklassificatie van Pasquill. Bij deze klassificatie wordt de stabiliteit van de onderste 50 m van de atmosfeer ingedeeld in zes klassen. De klassen beschrijven de toestand variërend van onstabiel tot stabiel in termen van de 10 m windsnelheid en de

bedekkingsgraad. Deze klassificatie is echter kwalitatief en nogal grof. Daardoor is de Pasquill-klassificatie alleen bij statistisch gebruik zinvol. Effecten van de terreingesteldheid op de stabiliteit kunnen niet direkt worden meegenomen. Boven water geldt de klassificatie in het geheel niet.

Bij het gebruik van het Gaussische pluimmodel wordt het windprofiel doorgaans beschreven met een machtwet met een vaste exponent voor elke stabiliteitsklasse. Onderzoek heeft echter aangetoond dat het machtwet profiel een te grove benadering is van de werkelijkheid. Dit komt omdat geen rekening wordt gehouden met de ruwheid van het onderliggende aardoppervlak en doordat variaties in de stabiliteit binnen een klasse niet worden verdisconteerd.

De menghoogte wordt in het lange termijn gemiddelde model op een vaste waarde gefixeerd voor elke stabiliteitsklasse [9]. De menghoogte kan in werkelijkheid echter sterk variëren bij dezelfde stabiliteitsklasse, bijvoorbeeld door de aanwezigheid van inversies en bewolking.

De conclusie van deze paragraaf is dan ook dat het huidige systeem alleen in statistische zin kan worden toegepast. Ook dan is het systeem nog steeds een grove benadering van de werkelijkheid. In het volgende zullen we een andere aanpak voorstellen die in principe meer mogelijkheden biedt.

4. Aanzet tot een verbeterde berekeningsmethode voor de verspreiding van luchtverontreiniging.

De beschrijving van de verspreiding van luchtverontreiniging kan alleen worden verbeterd als de toestand van de atmosfeer beter kan worden gekarakteriseerd. Zoals in paragraaf 2 werd beschreven is hiervoor allereerst nodig dat de ruwheid van het aardoppervlak bekend is. De ruwheidslengte z_o kan worden geschat uit een terreinbeschrijving of uit routinemetingen van de 10 m wind [18,25].

Verder zijn voor een verbeterde methodiek nodig de wrijvingssnelheid u_*, de voelbare warmteflux H, de grenslaagdikte h en de geowind G. Deze meteorologische grootheden moeten routinematig beschikbaar zijn voor praktische toepassing van een verbeterde beschrijving. In de hoofdstukken II en III van dit rapport wordt een praktische methode voor de bepaling van u_* en H boven land uit routinemetingen beschreven. In paragraaf 5 wordt een samenvatting van de voorgestelde methodiek gegeven. Boven een wateroppervlak is reeds een andere methode beschikbaar [11].

De grenslaagdikte h kan worden bepaald met behulp van metingen aan masten met ballonopstijgingen of met remote-sensing technieken. Modellering van h levert op dit moment nog problemen. Wel zijn er belangrijke vorderingen [2,14]. Op het KNMI is een praktisch model ontwikkeld dat thans in beperkte mate aan de praktijk is getoetst [16]. De resultaten zijn bevredigend overdag maar 's nachts zijn er nog grote afwijkingen. Een beter model voor de nacht is in een redelijk stadium van ontwikkeling. Het laat zich aanzien dat dit probleem binnen niet al te lange tijd kan worden opgelost.

De geowind G kan uit oppervlaktewaarnemingen van de druk worden bepaald [1]. Dit betekent uiteindelijk dat de belangrijke parameters die de toestand van de atmosfeer bepalen uit routinemetingen kunnen worden afgeleid. De volgende stap is de ontwikkeling van verspreidingsmodellen in termen van z_o, u_*, H, h en G. Ook hieraan is al het nodige werk verricht.

Verticale dispersie uit lage bronnen kan worden beschreven met een gelijkvormigheidsmodel [20] of met een zogenaamd K-diffusie model [4,12]. Verticale dispersie uit hoge bronnen kan ook worden beschreven met een K-diffusie model [15] of met statistische pluimmodellen [3]. Voor het praktisch bruikbaar maken is echter nog wel ontwikkelingswerk vereist.
Horizontale dispersie is nog een probleem. Slechts voor bepaalde omstandigheden zijn goede modellen voorhanden (zie bijvoorbeeld [13]). Met name in stabiele omstandigheden is het modelleren van horizontale dispersie problematisch.

Op grond van het bovenstaande kan worden gesteld dat lange termijn modellen, waarin horizontale dispersie geen rol speelt, in principe kunnen worden verbeterd. Hiervoor is echter nog wel ontwikkelingswerk vereist voordat praktische hanteerbaarheid gerealiseerd kan worden. Over de winst aan nauwkeurigheid kan pas echt iets worden gezegd als zo'n model in zijn geheel aan de praktijk kan worden getoetst. Het is echter wel te verwachten dat genoemde nauwkeurigheid zeker ten aanzien van hoge bronnen verbeterd kan worden.

5. Samenvatting van de voorgestelde methodiek voor de praktische bepaling van de wrijvingssnelheid en de voelbare warmtestroom met haar toepassingen.

Zoals hierboven werd betoogd is voor een betere beschrijving van de dispersie van luchtverontreiniging een praktische bepaling van de

wrijvingssnelheid u_* en de voelbare warmtestroom H essentieel. In hoofdstuk II van dit rapport wordt een methode gegeven voor de bepaling van u_* en H overdag in onstabiele omstandigheden [7]. Deze methode is gebaseerd op parameterizaties van de componenten in de stralingsbalans en de energiebalans aan het aardoppervlak. In hoofdstuk III wordt een empirische methode besproken voor de bepaling van de stabiliteit in stabiele omstandigheden ('s nachts en in overgangsuren) [6,24].

Bij de toepassing van de methodiek wordt gebruik gemaakt van de totale bedekkingsgraad van bewolking in de atmosfeer, de luchttemperatuur op 2 meter hoogte en de windsnelheid op 10 meter hoogte. Deze gegevens worden routinematig door het KNMI verzameld. De nauwkeurigheid van de schatting overdag kan worden vergroot door gebruik te maken van de gemeten kortgolvige straling. Deze grootheid wordt routinematig door het RIV en het KNMI gemeten. Deze versie van de voorgestelde methodiek heeft dan ook de voorkeur. Naast de meteorologische grootheden wordt in de methodiek gebruik gemaakt van enkele eigenschappen van het aardoppervlak. Overdag zijn het albedo en een vochtigheidsindikatie van het oppervlak vereist. Daarnaast wordt voor het gehele etmaal de ruwheidslengte van het oppervlak gebruikt. De ruwheidslengte kan eveneens uit standaard meteorologische waarnemingen bepaald worden [25].

De gehele methodiek is getoetst aan waarnemingen verricht aan de KNMI meetmast te Cabauw. Voor Nederlandse omstandigheden wordt een goede overeenkomst gevonden tussen de resultaten van de voorgestelde methodiek en de waarnemingen. De methodiek is zodanig opgezet dat eventuele nieuwe inzichten en ontwikkelingen gemakkelijk kunnen worden ingepast.

De voorgestelde methodiek wordt toegepast in het door het KNMI onwikkelde mesoschaal verspreidingsmodel van luchtverontreiniging [18]. Ook wordt de methodiek gebruikt in een grenslaagmodel gekoppeld aan trajectoriën van luchtmassa's [16]. In vereenvoudigde vorm is de methodiek toegepast ten behoeve van enige berekeningen bij de verspreiding van methylbromide in het Westland [17]. Momenteel wordt de methodiek toepasbaar gemaakt voor het schatten van de windsnelheid tot 80 meter hoogte [8]. Dit laatste is onder meer van belang voor de bepaling van de transportsnelheid van rookpluimen. Geconcludeerd kan worden dat de voorgestelde methodiek zijn nut al heeft bewezen voor het praktisch toepasbaar maken van moderne grenslaag- en luchtverontreinigingsmodellen.

Referenties

1. Cats, G.J. (1980): Analysis of surface wind and its gradient in a mesoscale wind observation network. Mon. Wea. Rev., 108, 1100-1107.

2. Driedonks, A.G.M. (1981): Dynamics of the well-mixed atmospheric boundary layer. KNMI Wetenschappelijk Rapport WR 81-2, De Bilt, 189 p.

3. Gryning, S.E. (1981): Elevated source SF_6-tracer dispersion experiments in the Copenhagen area. Report R-446, Risö, 187 p.

4. Gryning, S.E., Van Ulden, A.P., Larsen, S.E. (1982): Evaluation of a K-model formulated in terms of Monin-Obukhov similarity with the results of the Prairie grass experiments. Submitted to Quart. J. R. Met. Soc..

5. Holtslag, A.A.M. (1982): Estimates of vertical diffusion from sources near the ground in strongly unstable conditions. Preprints for the 13th International Technical Meeting on Air Pollution Modeling and its Application, Toulon, France.

6. Holtslag, A.A.M., Van Ulden, A.P. (1982): Simple estimates of nighttime surface fluxes from routine weather data. KNMI Wetenschappelijk Rapport WR 82-4, De Bilt, 11 p.

7. Holtslag, A.A.M., Van Ulden, A.P. (1983): A simple scheme for daytime estimates of the surface fluxes from routine weather data. Submitted to J. Appl. Meteor.

8. Holtslag, A.A.M. (1983): Estimation of the wind speed up to 80 m from routine weather data compared with observations. To be submitted to Boundary Layer Meteorol.

9. Kleine Commissie (1976): Modellen voor de berekening van de verspreiding van luchtverontreiniging. Staatsuitgeverij, Den Haag, 89 p.

10. KNMI (1979): Luchtverontreiniging en Weer, Staatsuitgeverij, Den Haag, 324 p.

11. Nieuwstadt, F.T.M. (1977): The dispersion of pollutants over a watersurface. Preprints for the 8th International Technical Meeting on Air Pollution Modelling and its Application, Louvain-la-Neuve, Belgium.

12. Nieuwstadt, F.T.M., Van Ulden, A.P. (1978): A numerical study on the vertical dispersion of passive contaminants from a continuous source in the atmospheric surface layer. Atmospheric Environment, 12, 2119-2124.

13. Nieuwstadt, F.T.M. (1980): Application of mixed-layer similarity to the observed dispersion from a ground-level source, J. Appl. Meteorol, 19, 157-162.

14. Nieuwstadt, F.T.M. (1981): The nocturnal boundary layer. Theory and experiments. KNMI Wetenschappelijk Rapport WR 81-1, De Bilt.

15. Ragland, K.W., Dennis, R.L.(1975): Point source atmospheric diffusion model with variable wind and diffusivity profiles. Atmospheric Environment, 9, 175-189.

16. Reiff, J., Van Ulden, A.P., Cats, G., Blaauboer, D., De Bruin, H.A.R. (1983): An air mass transformation model for short-range weather forecasting, Part I: The model. Submitted to Mon. Wea. Rev. (KNMI Memo DM-82-24).

17. Van Dop, H., Holtslag, A.A.M., Den Tonkelaar, J.F. (1981): Een waarschuwingsverwachting t.b.v. een vergunningsverleningsprocedure voor bodem ontsmetting met methylbromide. KNMI Technisch Rapport T.R.-6, De Bilt.

18. Van Dop, H., De Haan, B.J., Engeldal, C. (1982): The KNMI mesoscale air pollution model. KNMI Wetenschappelijk Rapport W.R. 82-6, De Bilt.

19. Van Ulden, A.P. (1974): On the spreading of a heavy gas released near the ground, 1st Int. Loss Prevention Symp., Den Haag, Elsevier.

20. Van Ulden, A.P. (1978): Simple estimates of vertical diffusion from sources near the ground. Atmospheric Environment, 12, 2125-2129.

21. Van Ulden, A.P., Holtslag, A.A.M. (1980): The wind at heights between 10 m and 200 m in comparison with the geostrophic wind. Seminar on radioactive releases, E.G., Risö.

22. Van Ulden, A.P., De Haan, B.J. (1981): Two-dimensional unsteady gravity currents. Reprints for the 12th International Technical Meeting on Air Pollution Modeling and its Application, Palo Alto, USA.

23. Van Ulden, A.P. (1981): Meteorologische aspecten van de verspreiding van luchtverontreiniging. In: Cursus Verontreiniging van de buitenlucht. Stichting Postacademiale Vorming Gezondheidstechniek.

24. Van Ulden, A.P., Holtslag, A.A.M. (1983): The stability of the atmospheric surface layer during nighttime. Preprints for the 6th Symposium on Turbulence and Diffusion, AMS, Boston.

25. Wieringa, J. (1980): Estimation of mesoscale and local-scale roughness for atmospheric transport modelling. Preprints for the 11th International Technical Meeting on Air Pollution Modelling and its Application, Amsterdam.

Hoofdstuk II

A simple scheme for daytime estimates of the surface fluxes from routine weather data.*

Abstract

In this paper a simple empirical scheme is presented, which gives hourly estimates of the surface fluxes of heat and momentum from routine weather data during daytime. The scheme is designed for grass surfaces, but it contains parameters which take account of the surface properties in general. The required input weather data are no more than a single wind speed, air temperature at screen height and total cloud cover. The output of the scheme is in terms of the Monin-Obukhov similarity parameters; it is obtained by using estimates for the mean values of the surface radiation and energy budget. For the climate of the Netherlands a good agreement is found between a full year of observations and estimates made with the scheme. For all data it appears that root mean square errors are σ = 90 Wm^{-2} for the incoming solar radiation, σ = 63 Wm^{-2} for the net radiation, σ = 34 Wm^{-2} for the sensible heat flux, σ = 0.01 ms^{-1} for the friction velocity and σ = 0.67 x 10^{-3} for the similarity ratio between the surface roughness length and the Obukhov stability parameter. A discussion is given on the surface parameters and coefficients of the scheme.

1. Introduction

The surface fluxes of heat, water vapor and momentum determine to a great extent the state of the atmospheric boundary layer. As such these fluxes are the principal boundary conditions for e.g. weather forecast models and air pollution dispersion models. In principle the fluxes can be measured. However, usually such measurements are not available, and in a forecast model the fluxes have to be parameterized in terms of variables predicted by the model. So in general there is a need to relate the surface fluxes to

* Referentie [7] van hoofdstuk I.

weather variables, either measured routinely or predicted by forecast models. It is the aim of this paper to establish such relations.

A scheme is developed that requires the following input data: total cloud cover, mean wind speed at one level and air temperature. Moreover estimates of the surface characteristics and of the solar elevation are used. If available, measurements of the global radiation can be included. The scheme provides estimates for the incoming solar radiation (K^+), the net radiation (Q^*), the flux of sensible heat (H), the evaporation rate (E), the surface stress in terms of the friction velocity (u_*) and the Obukhov stability parameter (L). As such the scheme can serve as an alternative for the traditional Pasquill stability classification (Pasquill, 1974).

The scheme consists of four parts which are described in the sections 2-5 (see also table 1). In section 2 we deal with the parameterization of the incoming solar radiation in terms of solar elevation and total cloud cover. We adopt the models by Collier and Lockwood (1974, 1975) and by Kasten and Czeplak (1980). We test these models on radiation data obtained in Cabauw and De Bilt.

In section 3 we present a model for the surface radiation budget which proceeds the net radiation. The model is a generalization of the model by Monteith and Szeicz (1961) and is tested against an independent data set. Section 4 describes the partitioning of the net radiation over the various heat fluxes at the earth's surface. We use the energy balance model by De Bruin and Holtslag (1982) with the net radiation estimated from the model of section 3. The calculated sensible heat flux is compared with the heat flux obtained from measured temperature and wind profiles (see appendix A).

Finally in section 5 we use the estimated heat flux in combination with a single wind speed to obtain the friction velocity (u_*) and the Obukhov stability parameter (L). We compare u_* and L with the values obtained directly from measured wind and temperature profiles (appendix A). In this section we use the Monin-Obukhov similarity theory for the atmospheric surface layer and the flux-profile relations by Dyer and Hicks (see Dyer, 1974 and Paulson, 1970).

In each section the output of the scheme is compared with meteorological observations in Cabauw, the Netherlands. A description of the Cabauw facilities can be found in Driedonks et al. (1978). For our comparisons we have used from a full year of available daytime data those, for which no instrumental or observational errors were reported and for which no rain, snow or fog appeared. Therefore the application of the scheme is restricted to neutral or unstable weather conditions, when the flux of sensible heat is positive.

The scheme is designed for grass surfaces, but it contains parameters which take account of the surface properties in general. This is discussed in section 6. Future refinements of the scheme are possible within the same general framework.

2. The incoming solar radiation.

At many meteorological stations, incoming solar radiation is measured. When such measurements are available, these can be used directly to estimate the net radiation (see section 3). When no measurements are at hand, observations of total cloud cover (N) and knowledge of the solar elevation (ϕ) are needed to estimate the incoming solar radiation. A simple procedure for the estimation of ϕ from the geographical position on earth and the time is given in appendix B. Here we present a method to determine the incoming solar radiation.

2.1. Clear skies.

The incoming solar radiation at ground level in clear skies (K_o^+) depends to a very large extent on the solar elevation ϕ. A simple parameterization for K_o^+ is (Kasten and Czeplak, 1980; Collier and Lockwood, 1974)

$$K_o^+ = a_1 \sin \phi + a_2 \ , \qquad (1)$$

where a_1 and a_2 are empirical coefficients. These coefficients describe the average atmospheric attenuation of K_o^+ by water vapour and dust for a given site.

In table 2 published values for the turbidity coefficients a_1 and a_2 are given for several locations. Also least square estimates of a_1 and a_2 are given for clear sky data in De Bilt in 1977. These data were obtained with a Moll-GorczynsRi pyranometer for 504 hours with total cloud cover $N \leq 0.25$ and solar elevation $\phi > 10$ degrees.

It appears that for the same value of ϕ the coefficients of table 2 give a broad range of average K_o^+ values. This range can be attributed to climatological variations in the turbidity of the atmosphere. The coefficients of Collier and Lockwood (1975) give a fair average of all coefficients for $\phi > 20$ degrees. Therefore the latter coefficients can be used for a site where the turbidity coefficients are not known at beforehand, which is usually the case. Then we may expect systematic deviations for K_o^+ up to about 10% depending on the mean turbidity of the site. The accuracy of the mean solar radiation estimates at clear skies is also within about 10%.

Apart from mean deviations also random deviations will occur due to local variations in the turbidity. To get an impression of the total error which have to be expected we have made a comparison of (1) with observations or K_o^+ in De Bilt and Cabauw, The Netherlands. The calculations were made with the coefficients of Collier and Lockwood (1975) for cases with solar elevation $\phi > 10$ degrees. Results are given in tables 3a and 3b. Table 3a shows at the left hand side the comparison for De Bilt at clear skies ($N < 0.25$). It is seen that the agreement is good. The root mean square error $\sigma = 46.7$ Wm^{-2}, which is 11% of the observed average. When our adjusted values for De Bilt ($a_1 = 1041$ Wm^{-2} and $a_2 = -69$ Wm^{-2}) are used the agreement improves, of course ($\sigma = 40$ Wm^{-2}). From table 3b for the comparison at Cabauw we obtain $\sigma = 54.8$ Wm^{-2}, which is 13% of the observed average. In the following we will use (1) with the coefficients of Collier and Lockwood (1975). Then for our data in The Netherlands the total error in the incoming solar radiation at clear skies is within 13% on average.

2.2. The effect of clouds

In general the presence of clouds reduces the incoming solar radiation. Many publications have appeared on this subject. Often a distinction is made between the amount of higher and lower clouds and between the types of clouds (e.g. Davies and Uboegbulam, 1979). Other models use the total cloud cover only; e.g. Kasten and Czeplak (1980) propose

$$K^+ = K_o^+ (1 + b_1 N^{b_2}), \qquad (2)$$

where N is total cloud cover, K_o^+ is the value from (1) and b_1 and b_2 are empirical coefficients, which may depend on the climate of the specific site. Kasten and Czeplak obtain for 10 years of observations at Hamburg $b_1 = -0.75$ and $b_2 = 3.4$ on the average. With b_1 and b_2 of Kasten and Czeplak, and a_1 and a_2 of (1) taken from Collier and Lockwood (1975), we have made a comparison of (2) with one year of pyranometer measurements of K^+ in De Bilt and Cabauw. We have used hourly and 30-minute averages for solar elevation $\phi \geq 10$ degrees. The results are summarized in tables 3a and 3b. In these tables we have distinguished three classes of total cloud cover (N). In table 3a for data at De Bilt, it is seen that the ratio between the root mean square error and the observed average increases from 11% at clear skies ($N \leq 0.25$), and ~ 24% at intermediate cloud fractions ($0.25 < N < 0.75$), up to ~ 37% for cloudy skies ($N \geq 0.75$). These findings reflect the problems by estimating shorttime values for K^+ from cloud data, such as the possible overlap of different type of clouds, the position of the clouds with respect to the direct solar beam, the varying atmospheric turbidity, etcetera.

From table 3b for the data at Cabauw it is seen that the scatter increases slightly compared with the results of table 3a. Probably this is caused by the averaging of total cloud cover observed at four weather stations around Cabauw, which was done because no local cloud observations were available in Cabauw. In Fig. 1 a random selection of the comparison for Cabauw is given. Here only two classes of cloud cover are distinguished. From the skill of Fig. 1, which is representative for the whole data set of

table 3b, it is seen that large deviations can occur between (1) and (2) and observations. However, in general the simple estimates of (1) and (2) may still be useful in practice, as will be shown in the following.

3. The surface radiation budget.

To estimate the net radiation Q^* at the surface we parameterize the components of the surface radiation budget. This reads:

$$Q^* = (1 - r)K^+ + L^+ - L^- \quad , \tag{3}$$

where r is the albedo of the surface, L^+ the incoming longwave radiation from the atmosphere and L^- the outgoing longwave radiation from the surface. K^+ is the incoming solar radiation that we have discussed in the former section. Of this radiation a fraction r is reflected by the surface. This fraction depends on the type of the surface, the solar elevation and the shortwave spectrum (Paltridge and Platt, 1976). From measurements in Cabauw over short grass we found r = 0.23 on the average. This is a normal value for short grass (Oke, 1978). We will use this constant value for r (see section 6.1). In the following we are dealing with the two longwave terms of (3), L^+ and L^-, to obtain finally Q^* .

3.1. The incoming longwave radiation L^+.

A very simple parameterization of the incoming longwave radiation in the absence of clouds L_o^+ was proposed by Swinbank (1963). He related L_o^+ to the air temperature T at screen height (1-2 m) by

$$L_o^+ = c_1 T^6 \quad , \tag{4}$$

where $c_1 = 5.31 \times 10^{-13}$ $Wm^{-2}K^{-6}$ is an empirical constant. Arnfield (1979) tested this relation for several locations and concluded, that its estimate is within 5 percent on the average. We will adopt this relation for clear skies. To account for cloud cover (N), we

employ the linear correction by Paltridge and Platt (1976). This reads:

$$L^{+} = c_1 T^6 + c_2 N \ , \qquad (5)$$

where $c_2 = 60\ Wm^{-2}$ is appropriate for mid-latitudes.

Other type of parameterizations of L^{+} are discussed in Arnfield (1979) and Lind and Katsaros (1982).

3.2. The outgoing longwave radiation L^{-}.

The outgoing longwave radiation L^{-} from the surface arises from the Stefan-Boltzmann law

$$L^{-} = \sigma T_s^4 \ , \qquad (6)$$

where the earth's surface is assumed to be a black body (Sellers, 1965), $\sigma = 5.67 \times 10^{-8}\ Wm^{-2}K^{-4}$ is the Stefan-Boltzmann constant and T_s is the surface radiation temperature. Since the surface radiation temperature is not normally available we approximate L^{-} by

$$L^{-} = \sigma T^4 + 4\sigma T^3 (T_s - T) \ . \qquad (7)$$

During unstable conditions the surface radiation temperature T_s exceeds the air temperature T. To obtain a suitable description of the correction term $4\sigma T^3 (T_s - T)$ in (7) we made a comparison between measurements of this term and measurements of the incoming solar radiation K^{+}, the net radiation Q^{*} and the sensible heat flux H obtained with the Bowen's ratio method (see section 4 and Oke, 1978). For this comparison we use data of our micrometeorological field at Cabauw. This field is covered with short grass (kept at ~ 8 cm). The surface radiation temperature T_s was measured with a infra-red radiation thermometer (type Heimann). The air temperature is measured at 1.1 m.

Fig. 2 shows results of the comparison for four days in the summer of 1977, where we have used 30-minute averages. For these days the total cloud cover N varied between N = 0.25 and N = 1,

while the average value was $N \simeq 0.5$. Further the average wind speed at 10 m varied between $U_{10} \simeq 2.5$ ms^{-1} and $U_{10} \simeq 6$ ms^{-1}, with an average $U_{10} \simeq 4$ ms^{-1}. From the comparison between $4\,\sigma T^3\,(T_s-T)$ and K^+, Q^* and H no wind speed effect and no cloud cover effect could be detected. From Fig. 2 it is seen that a good estimate of the correction term in (7) can be obtained from Q^*, so that

$$4\,\sigma T^3\,(T_s-T) = c_3\,Q^*, \tag{8}$$

is a good approximation. From the limited amount of data in Fig. 2b we obtained $c_3 \simeq 0.12$. Since (8) and c_3 describe the relative increase of the surface radiation temperature with net radiation c_3 may be regarded as a heating coefficient for the surface (see also Monteith and Szeicz, 1961). In section 6.4. we will discuss the heating coefficient in more detail. With (7) and (8) we can approximate L^- by

$$L^- = \sigma T^4 + c_3\,Q^* . \tag{9}$$

3.3. The net radiation Q^*.

When we use (5) for the incoming longwave radiation L^+ and (6) for the outgoing longwave radiation L^- we obtain for Q^* from the surface radiation budget (3)

$$Q^* = (1-r)\,K^+ + c_1 T^6 - \sigma T_s^{\,4} + c_2\,N . \tag{10}$$

Here is is seen that Q^* is in general a function of K^+ and r as pointed out before. Moreover Q^* depends on the air temperature at screen height T, the surface radiation temperature T_s, the total cloud cover N and the coefficients c_1 and c_2. Because T_s is not a routine weather quantity, we approximate L^- by (9) instead of (6), which yields for Q^*

$$Q^* = \frac{(1-r)\,K^+ + c_1\,T^6 - \sigma T^4 + c_2\,N}{1 + c_3} . \tag{11}$$

We have compared (11) with one year of 30-minute measurements

of Q^* obtained with a Suomi net pyrradiometer in Cabauw. The estimates are made using r = 0.23 and c_3 = 0.12, both with measured values of K^+ and with K^+ estimated by means of (1) and (2). Table 4a shows the results for the calculation with measured K^+. Again a distinction is made in three classes of total cloud cover. It is seen that the root mean square error normalised by the observed average is within 10% for $N \leq 0.75$ up to 12.4% at cloudy skies Fig. 3 shows for a random sample of the data in table 4a the good agreement for Q^*.

Table 4b shows the results for Q^* with calculated values of K^+ from (1) and (2). Thus only air temperature and total cloud cover are used as input weather data to obtain Q^*. For clear skies ($N \leq 0.25$) the scatter increases only slightly with respect to table 4a. But for larger cloud amounts the normalised error increases from ~ 28% at intermediate cloud covers ($0.25 < N < 0.75$) up to ~ 35% for cloudy skies ($N > 0.75$). This is caused by the errors in the estimation of K^+ with (1) and (2). However, the estimate of Q^* is still satisfactory.

In the present model the properties of the surface are represented by two adjustable parameters. The first parameter is the albedo r, which describes the effect on the net incoming solar radiation. The second parameter c_3 characterizes the thermal properties of the surface. Thus the present approach is fairly general. It has the advantage that the basic physics of the surface radiation budget are still present in the final parameterization. This in contrast with the regression models used by Monteith and Szeicz (1961), Gay (1971) and Nielsen et al. (1980). In the latter models regressions are made between net incoming solar radiation $(1 - r)K^+$ and the net radiation Q^*. In such an approach specific site effects are not so easy to recognize. In the present approach these can be dealt with in principle (see section 6.4).

4. The surface energy budget.

The surface energy budget relates the net radiation Q^* of the former section to the various heat fluxes at the earth's surface.

This reads (Oke, 1978):

$$H + \lambda E + G = Q^* \quad , \tag{12}$$

where H is the sensible heat flux, λE the latent heat flux and G is the soil heat flux. For a land surface G is mostly small compared with Q^* during daytime. A good estimate for G is (De Bruin and Holtslag, 1982)

$$G = c_G Q^* \quad , \tag{13}$$

where $c_G = 0.1$ is obtained for a grass covered surface in the Netherlands (see also section 6.2).
Since net radiation can be evaluated from standard meteorological data (section 3), the partitioning of H and λE over the available energy $Q^* - G$ has to be dealt with.

4.1. The partitioning of H and λE.

A physically realistic way to determine the partitioning of H and λE is the Penman-Monteith approach (Monteith, 1981). A problem with this approach is that it is complicated, and that several input parameters are needed which are difficult to obtain. For instance, the surface resistance for latent heat is needed. Several attempts are made in literature to evaluate this surface resistance by means of empirical rules (Smith and Blackall, 1979; Deheer-Amissah et al., 1981; Berkowicz and Prahm, 1982). However, De Bruin and Holtslag (1982) show that the Penman-Monteith approach can be simplified in such a way that it becomes more suitable in the present context.

The simplified parameterization reads:

$$H = \frac{(1 - \alpha) + (\gamma/s)}{1 + (\gamma/s)} (Q^* - G) - \beta \quad , \tag{14}$$

and

$$\lambda E = \frac{\alpha}{1 + (\gamma/s)} (Q^* - G) + \beta \quad . \tag{15}$$

Here $s = \partial q_s/\partial T$, where q_s is the saturation specific humidity; $\gamma = C_p/\lambda$, where C_p the specific heat of air at constant pressure and λ the latent heat of water vaporization; α and β are empirical parameters. The ratios γ/s and $(\gamma/s)/(1+\gamma/s)$ are tabulated as a function of temperature at standard pressure in table 5.

To evaluate H and λE by way of (14) and (15) we must specify α and β. The parameter α accounts for the (strong) correlation of H and λE with $Q^* - G$, while the parameter β accounts for the uncorrelated part. Both α and β may depend on the surface moisture condition. Preliminary estimates for a grass covered surface in the Netherlands are $\alpha \simeq 1$ and $\beta \simeq 20$ Wm^{-2} (De Bruin and Holtslag, 1982).
These values are obtained for normal summer conditions, when the surface is supplied with enough water to evaporate. When there is lack of water the value of α decreases (De Bruin and Holtslag, 1982). Since in the Netherlands the surface is normally not very dry, $\alpha = 1$ and $\beta = 20$ Wm^{-2} should be good enough for our practical scheme; we will use these values below. In section 6.3 we discuss values of α and β for other surface moisture conditions.

4.2. Estimation of the sensible heat flux.

In this section we will compare the flux of sensible heat calculated with (11), (13) and (14) with the heat flux derived from measured wind and temperature profiles. The estimation of the heat flux has been performed both with measured incoming solar radiation K^+ (table 6a) and with the calculated value using (1) and (2) (table 6b). The "observed" heat flux was obtained from a full year of profile data in unstable conditions (30-minute averages) with the semi empirical flux-profile relations by Dyer and Hicks (see Appendix A).

From table 6a it is seen that the root mean square error normalised by the observed average increases slightly with total cloud cover from ~ 43% for clear skies ($N \leq 0.25$) up to ~ 48% for $N > 0.75$. Fig 5 shows a random sample of the data in table 6a. From table 6b it is seen that the normalised error increases from ~ 48% for clear skies ($N \leq 0.25$) up to ~ 70% for cloudy skies

($N \geq 0.75$), when estimates of K^+ are used from (1) and (2). Fig. 6 shows a sample of the data in table 6b. From the tables and figures it is clear that with measurements of K^+ the estimates of H are improved.

The relative skill of H improves with increasing instability. For 179 selected cases with $-100 \leq L < 25$ m we obtain $\sigma = 40$ Wm^{-2}, which is 49% of the observed average. Here L is the Obukhov stability parameter (see section 5). When measurements of K^+ are used we obtain $\sigma = 34$ Wm^{-2} which is 42% of the observed average in the selected very unstable cases.

In the above calculations we have used $\alpha = 1$ and $\beta = 20$ Wm^{-2} under all circumstances. The specific dependence of α and β on the moisture condition of the surface awaits further examination and should improve the performance of the scheme (see also section 6.3). Nevertheless, even with constant values for α and β the accuracy of the present scheme is quite satisfactory. This is illustrated in the following by a comparison between heat fluxes obtained from measurements using two different methods at two sites in Cabauw which are close to each other.

The first method is the Bowen's ratio method, in which measurements of the net radiation and the soil heat flux are used together with the ratio of the sensible heat flux to the latent heat flux (see Oke, 1978). The ratio between the fluxes is derived from observed profiles of temperature and humidity. The second method is the earlier mentioned flux-profile method of appendix A. The comparison between the two "observed" heat fluxes is shown in Fig. 7. The data of Fig. 7 were obtained during the summer of 1977. In general the agreement between the two methods in Fig. 7 is good, but the skill is only slightly better than of Fig. 5. This is due to measurement errors, to small scale terrain variations and to physical imperfections in the two methods. Fig. 7 shows the limited accuracy in obtaining H from measurements. Therefore we conclude

that (14) with $\alpha = 1$ and $\beta = 20$ Wm^{-2} produces in general rather good estimates for hourly values of H.

In appendix C an application of the scheme for H is given. There the solar elevation is calculated for transition hours between stable and unstable conditions, when H vanishes.

5. The momentum flux and the Obukhov stability parameter.

Knowing the heat flux from the preceding part of our scheme, it is a small step to estimate the Obukhov stability parameter L and the surface momentum flux or shear stress. The latter quantity is normally denoted by

$$\tau = \rho u_*^2 , \qquad (16)$$

where ρ is the density of air and u_* the friction velocity. Applying Monin-Obukhov similarity theory, u_* is related to the wind speed U_z at the height z by (see Dyer, 1974 and Paulson, 1970)

$$u_* = kU_z \left[\ln(z/z_o) - \psi_M(z/L) + \psi_M (z_o/L)\right]^{-1} , \qquad (17)$$

where k is the Von Kármán constant ($k = 0.41$), z_o the surface roughness length, ψ_M a stability function (defined in appendix A) and

$$L = - \frac{\rho C_p T u_*^3}{k g H} , \qquad (18)$$

the Obukhov stability parameter. Here T is the air temperature, g the acceleration of gravity, ρ the density of air, C_p the specific heat at constant pressure, and H is the sensible heat flux.

From (17) and (18) u_* and L can be solved by iteration when T, H, z_o and U_z are known. The surface roughness length (z_o) can be obtained from table 7 (see also section 6.5). To solve u_* and L we use the following procedure. The sensible heat flux H is estimated with (11), (13), (14) and measurements of K^+ or estimates of K^+ with (1) and (2). The measured 10 m wind speed is used for U_z and for T the air temperature at screen height (2 m) is used. The computation

starts with an estimate for u_* by way of (17), where we take initially $\psi_M = 0$ ($L = \infty$). Then with (18) an estimate for L is obtained. With this estimate again (17) is used to improve the estimate for u_*, and so on. It appears that usually not more than three iterations are needed to achieve an accuracy of 5 % in successive values of L.

Using the above procedure we obtain very good results for the friction velocity u_*. Notably the correlation coefficient between estimates and values derived from profiles (see appendix A) $r = 0.99$ and the root mean square $\sigma = 0.01$ ms^{-1}, which is 1.7% of the observed average. The results for z_o/L are $r = 0.85$ and $\sigma = 0.67 \times 10^{-3}$ which is 82% of the observed average. Here we have used the estimated value for the incoming solar radiation K^+ with (1) and (2) for the whole data set (number of observations $n = 999$).
A random selection of the data for z_o/L is given in Fig. 8. It is seen that the agreement for clear skies and cloudy skies is comparable.

In section 4.2 we have seen that the relative skill for H improves with increasing instability. As a result also the relative skill of z_o/L improves. For the 179 very unstable cases with $-100 \leq L < -25$ or $-6 \times 10^{-3} < z_o/L \leq -1.5 \times 10^{-3}$ (see section 6.5) we obtain $\sigma = 1.02 \times 10^{-3}$, which is ~ 40% of the observed average. When measurements of K^+ are used in the scheme we obtain $\sigma = 0.83 \times 10^{-3}$, which is ~ 33% of the observed average.

Certainly there will be some bias in the above comparison, since in both measured values of u_* and L and estimated values of u_* and L the same wind speed data have been used (Hicks, 1981). However, it has been shown earlier that our profile measurements relate well to direct eddy correlation measurements of u_* (Nieuwstadt, 1978). With this in mind we can still conclude from the above comparison, that with our scheme realistic estimates of u_* and L can be obtained.

6. Discussion on the surface parameters of the scheme.

6.1. The surface albedo r.

The albedo r describes the effect of the surface on the net incoming solar radiation, which is important in the surface radiation budget (3). In this study we have used a representative value for r of short grass. A more detailed evaluation of the albedo may take into account the dependence on solar elevation and the shortwave spectrum (Paltridge and Platt, 1976; Oke, 1978). In Oke (1978) and Burridge and Gadd (1977) values of r for other type of surface coverages can be found.

6.2. The ratio between soil heat flux and net radiation.

The ratio between soil heat flux and net radiation c_G is during the day only small compared with 1. We have used $c_G = 0.1$, which was obtained for a grass covered surface in the Netherlands (De Bruin and Holtslag, 1982). From measurements of the soil heat flux G and net radiation Q^* during the Prairie Grass experiment (Barad, 1958) we have found that with $c_G = 0.1$ good results can be obtained. The root mean square error between measurements and estimates of G is $\sigma = 27$ Wm^{-2}, which is 7% of the observed average of $Q^* - G$ in the Prairie Grass experiment. Also, Burridge and Gadd (1977) use $c_G = 0.1$ for snow-free surfaces if $Q^* > 0$. For snow-covered surfaces Burridge and Gadd propose $c_G = 0$, which reflects the poor conductivity of snow.This suject requires further investigation.

6.3. The surface moisture parameters α and β.

In section 4 we have introduced the surface moisture parameters α and β. We have seen that with $\alpha = 1$ and $\beta = 20$ Wm^{-2} good resuls for the sensible heat flux H can be obtained for grass provided with enough water to evaporate. In this section we will discuss values for α and β for other surface moisture conditions.

For bare soil, for instance, we expect $\lambda E = 0$ when there is no water to evaporate. In (14) and (15) α and β are constants for given surface conditions. This can only be fulfilled by putting

$\alpha = \beta = 0$ for $\lambda E = 0$. Taking these limits for α and β we may rewrite β of (14) and (15) as

$$\beta = \beta' \alpha \ , \tag{19}$$

where β' is the value for which $\alpha = 1$. Eq. (19) is in agreement with the value of β used in section 4 if $\beta' = 20$ Wm^{-2}.

In general we may rewrite (15) for λE with the use of (19) as

$$\lambda E = \alpha\{\frac{1}{1+\gamma/s} (Q^* - G) + \beta'\} \ . \tag{20}$$

In general α can be computed by means of a regression analysis between observations of λE and $(Q^*-G)/(1+\gamma/s) + \beta'$. For instance for the Prairie Grass experiment (see Barad, 1958), we obtain $\alpha = 0.45$ if $\beta' = 20$ Wm^{-2} (correlation coefficient $r = 0.6$, root mean square error $\sigma = 56$ Wm^{-2} for λE, which is 40% of the observed average).

The advantage of (20) is that in principle only one parameter remains which depends on the surface moisture condition (notably α). The specific dependence of α on the moisture condition of the surface awaits further examination.

6.4. The surface heating coefficient.

The surface heating coefficient c_3 of section 3.2 relates the difference between the surface radiation temperature T_s and the air temperature T to the net radiation Q^* as given in (8). On the other hand it is common practice to relate a surface temperature T_o and a air temperature T by (e.g. Monteith, 1981)

$$T_o - T = \frac{R}{\rho C_p} H \ . \tag{21}$$

Here R is the resistance for the flux of sensible heat H. In general R combines an atmospheric resistance and a surface resistance. The atmospheric resistance may depend on stability, wind speed, etcetera, as discussed by Thom and Oliver (1977). The surface resistance for sensible heat is still a matter of

controversy (Garratt and Hicks, 1973).

The surface radiation temperture T_s of (8) may differ from the surface temperature T_o of (21). In the present context we need a relation between $T_s - T$ and H. According to Fig. 2b it is seen that $4\sigma T^3(T_s - T) \simeq 0$ for $Q^* = 0$, which with (13) and (14) yields $H + \beta = 0$. These findings suggest that (21) can be changed into

$$4\sigma T^3(T_s - T) = \frac{4\sigma T^3 R'}{\rho C_p} (H + \beta) , \qquad (22)$$

where R' is a modified resistance for sensible heat. In Fig. 2c we have compared $4\sigma T^3(T_s - T)$ with H. From this limited amount of data no possible wind speed influence could be detected. Apparantly R' is dominated by transfer processes in the surface vegetation layer.

When (22) is combined with (8), (13) and (14), we may write for the surface heating coefficient c_3

$$c_3 = \frac{4\sigma T^3 R'}{\rho C_p} (1 - c_G) \left(\frac{1-\alpha + \gamma/s}{1 + \gamma/s}\right) . \qquad (23)$$

This relation shows that c_3 may vary with the surface moisture parameter α. Further it is seen that soil properties are important (accounted for by R' and c_G) and the air temperature T. In section 3.2 we have used $c_3 = 0.12$, which was obtained from the data of Fig. 2b. With this value of c_3 very good results for Q^* were obtained, as shown in Fig. 3 and table 4a. Using our values for c_3, c_G, α and $T = 15\ ^oC$ (average temperature) we obtain $R' \simeq 80\ sm^{-1}$. The latter estimate is on the average in agreement with the data of Fig. 2c.

Let us finally compute values of the heating coefficient c_3 for other surface and climatic conditions. For instance, for the Prairie Grass experiment (Barad, 1958) we obtain $c_3 = 0.25$. This value is calculated with (23) using $\alpha = 0.45$ (section 6.2), $T = 27\ ^oC$ (average value for the Prairie Grass experiment), $c_G = 0.1$ and $R' = 80\ sm^{-1}$. Further for bare soil we obtain $c_3 = 0.38$, using $\alpha = 0$, $c_G = 0.1$, $R' = 80\ sm^{-1}$ and $T = 27\ ^oC$.

The computed values of c_3 with (23) for the Prairie Grass

experiment and bare soil agree surprisingly well with the values reported by Monteith and Szeicz (1961). Their values were obtained from a regression analysis between Q^* and $(1-r)K^+$ at clear skies. The above findings seem to indicate that (23) can be used for estimates of c_3 for short vegetation with $R' = 80\ sm^{-1}$, $c_G = 0.1$ and varying values of α.

6.5. The surface roughness length z_o.

The surface roughness length z_o can be obtained from routine wind measurements with a method given by Wieringa (1976, 1980, 1983). This method relates z_o either to the normalized standard deviation of wind speed, or to the ratio of the averaged wind speed observed in a given period and the maximum gust recorded during the same period. If no gustiness observations are available, a crude estimate of z_o can be obtained from a visual terrain classification (table 7).

For our experimental site in Cabauw it appears that z_o varies with wind direction between $z_o = 0.06$ m and $z_o = 0.25$ m, with a typical value of $z_o = 0.15$ m on average.

7. Summary and conclusions

In this paper a simple empirical scheme is presented which relates the surface fluxes of heat and momentum to weather variables, either measured routinely or predicted by forecast models. The required input weather data are the air temperature, the total cloud cover and a single wind speed. The scheme is designed for a grass covered surface, but it contains parameters that can be adjusted to other coverages. An estimation scheme for the solar elevation is given which uses geographical position and time.

In the scheme the mean values of the surface radiation and energy budget are parameterized to obtain the sensible heat flux. From the sensible heat flux, a single wind speed and the surface roughness length, the flux of momentum in terms of the friction velocity is obtained, applying Monin-Obukhov similarity theory. The output of the scheme is compared with micrometeorological data, and

finally the fluxes are compared with fluxes derived from profile data in unstable conditions.

For one year of observations at Cabauw, The Netherlands, we obtain a good agreement between observations and estimates. It appears that the root mean square error σ = 90 Wm^{-2} for the incoming solar radiation, σ = 63 Wm^{-2} for the net radiation, σ = 34 Wm^{-2} for the sensible heat flux, σ = 0.01 ms^{-1} for the friction velocity and σ = 0.67 x 10^{-3} for the similarity ratio between the surface roughness length and the Obukhov stability parameter (z_o/L). Moreover the scheme provides the latent heat flux. The results for the net radiation and the sensible heat flux are improved markedly when measured values for the incoming solar radiation are used.

Because of its simplicity and its fair agreement with observations we conclude that the scheme is useful for many applications in boundary layer meteorology. At present the scheme is applied in the Dutch air mass transformation model for short range weather forecasting (Reiff et al., 1983) and in the K.N.M.I. mesoscale air pollution transport model (Van Dop et al., 1982).

Acknowledgements

The authors are grateful to Mr. H.R.A. Wessels for providing the solar elevation procedure (appendix B) and to Mr. J.Q. Keijman for providing the surface temperatures of the infra-red thermometer. Dr. H.A.R. De Bruin is thanked for providing the energy budget data of the micrometeorological field at Cabauw and for useful suggestions. Comments on the draft of this paper by Drs. H. Tennekes and J. Wieringa are gratefully acknowledged. This study was supported by the Dutch Ministry of Health and Environmental Protection.

Appendix A. Fluxes and profiles.

The fluxes of heat and momentum can be obtained from observed profiles of wind and temperature using the similarity relations for the atmospheric surface layer (see Dyer, 1974). These relations are based on Monin-Obukhov similarity theory, which assumes stationary and horizontally homogeneous conditions. The flux of momentum τ is related to the friction velocity u_* by

$$\tau = \rho\, u_*^2 \,, \tag{A1}$$

where ρ is the density of air. The flux of sensible heat H is related to u_* and the temperature scale θ_* by

$$H = -\rho\, C_p\, u_*\, \theta_* \,, \tag{A2}$$

where C_p is the specific heat at constant pressure. Nieuwstadt (1978) gives a method based on least square estimates, which provides u_* and θ_* from observed wind and temperature profiles. Then the fluxes can be calculated from (A1) and (A2). However, this method is rather complicated and time consuming.

In the following a simplified method is given of which the results are comparable to those from Nieuwstadt's method. We will use the simplified method to compare the fluxes with the fluxes of the proposed scheme in this paper. For the simplified method are needed: a single wind speed U_z at level z, a surface roughness length z_o and a temperature difference $\Delta\theta$ between two heights z_1 and z_2 in the atmospheric surface layer. With these data u_* and θ_* can be calculated from the integrated flux-profile relations of Dyer and Hicks (see Dyer, 1974 and Paulson, 1970)

$$u_* = k\, U_z \left[\ln\left(\frac{z}{z_o}\right) - \psi_M\left(\frac{z}{L}\right) + \psi_M\left(\frac{z_o}{L}\right)\right]^{-1} \tag{A3}$$

and

$$\theta_* = k\, \Delta\theta \left[\ln\left(\frac{z_2}{z_1}\right) - \psi_H\left(\frac{z_2}{L}\right) + \psi_H\left(\frac{z_1}{L}\right)\right]^{-1} . \tag{A4}$$

Here k is the Von Kármán constant, taken at k = 0.41, and L is the Obukhov stability parameter defined by

$$L = \frac{T\, u_*^2}{k\, g\, \theta_*} , \qquad (A5)$$

where g is accelaration of gravity and T is air temperature.
For L < 0 (unstable) it reads:

$$\psi_M = 2\, \ln\left(\frac{1+x}{2}\right) + \ln\left(\frac{1+x^2}{2}\right) - 2\, \tan^{-1}(x) + \frac{\pi}{2} \qquad (A6)$$

$$\psi_H = 2\, \ln\left(\frac{1+x^2}{2}\right) , \qquad (A7)$$

where

$$x = \left(1 - 16\, \frac{z}{L}\right)^{\frac{1}{4}} . \qquad (A8)$$

The fluxes H and τ can be obtained from the above equations starting with a prescribed value of the Obukhov stability parameter L. We have used L = -36. Then u_* and θ_* are calculated from (A3)-(A8). Using (A5), L is computed by using the estimated values of u_* and θ_*. The new value of L is substituted in (A3)-(A8) to obtain improved values for u_* and θ_*. This cycle is repeated until successive values of L do not change more than 5 %. It appears that only very few cycles are needed (usually not more than 3) in order to achieve the required accuracy of 5 % for L. Then H and τ are calculated with (A1) and (A2).

As input data we have used 30-minute averages of wind speed U_z at z = 10 m and the temperature difference $\Delta\theta$ between z_2 = 10 m and z_1 = 0.6 m from each second half hour of our data. The surface roughness length z_o was obtained from gustiness, using a method by Wieringa (1976; see section 6.5).
It appears that this simplified method provides fluxes which are within a few percent to the results of Nieuwstadt, (1978).

Appendix B. Procedure for estimating the solar elevation (ϕ).

The solar elevation (ϕ) for a given time and location may be calculated by simplifying well-known astronomical formulae. For a given day the daynumber d may be crudely estimated from

$$d = 30\ (M-1) + D\ , \qquad (B1)$$

where M is the number of the actual month (1-12) and D is the number of the actual day in the month (1-31). From d the solar longitude (SL) can be evaluated

$$SL = 4.871 + 0.0175d + 0.033 \sin (0.0175\ d)\ , \qquad (B2)$$

where SL is in radians. The solar declination (δ) follows from

$$\delta = \text{arc sin}\ (0.398 \sin (SL))\ . \qquad (B3)$$

Using the above estimates for d, SL and δ we can compute the hour angle (h) through which the earth must turn to bring the meridian of the given location directly under the sun

$$h = -\lambda_w + 0.043 \sin (2SL) - 0.033 \sin(0.0175\ d) + 0.262\ t - \pi\ , \qquad (B4)$$

where λ_w is the western longitude (in radians) of the location and t is the universal time in hours. The solar elevation (ϕ) follows from the above relations by applying (Sellers, 1965)

$$\sin(\phi) = \sin\delta \sin\psi + \cos\delta \cos\psi \cos h \qquad (B5)$$

where ψ is the latitude of the location (in radians).
With the above scheme for the calculation of ϕ the accuracy of ϕ is within 0.05 radians, which is acceptable within the present context.

Appendix C. The solar elevation for which the surface heat flux vanishes.

The solar elevation ϕ_o for which the boundary layer changes from a stable to an unstable stratification can be calculated from the proposed scheme. To this end H is taken zero in (14) and Q^* is solved using (13). From the obtained value for Q^* we calculated K^+ from (11) and finally ϕ_o from (1) and (2). We have selected hours with the actual solar elevation ϕ for which the absolute value of $(\phi-\phi_o) < 5$ degrees and for which the sensible heat flux from profiles (see appendix A) $H < 20$ Wm^{-2}.

Table 8 gives average results for the solar elevation ϕ_o and the observed and calculated values of the sensible heat flux within each class of total cloud cover (N). It is seen that the transition between stable and unstable conditions on the average takes place for $\phi_o \simeq 13$ degrees if $N < 0.75$, but that ϕ_o increases to 23 degrees for overcast conditions (N = 1).

On the average ϕ should exceed the values of ϕ_o listed in table 8 to obtain an unstable atmospheric surface layer. For instance, during wintertime in the Netherlands it is possible to obtain stable conditions during the whole day if the sky is overcast.

References

Arnfield, A.J., 1979: Evaluation of empirical expressions for the estimation of hourly and daily totals of atmospheric longwave emissions under all sky conditions. Quart. J. Roy. Met. Soc., 105, 1041-1052.

Barad, M.L., Ed., 1958: Project Prairie grass, a field program in diffusion. Geophys. Res. Rap. no. 59, Vol. I and II. Geophysics Research Directorate, Bedford.

Berkowicz, R. and L.P. Prahm, 1982: Sensible heat flux estimated from routine meteorological data by the resistance method. J. Appl. Meteor., 21, 000-000 (accepted for publication).

Burridge, D.M. and A.J. Gadd, 1977: The Meteorological Office Operational 10-level Numerical Weather Prediction Model. Scientific Paper 34, Meteor. Office London, 39 pp.

Collier, L.R. and J.G. Lockwood, 1974: The estimation of solar radiation under cloudless skies with atmospheric dust. Quart. J. Roy. Met. Soc., 100, 678-681.

Collier, L.R. and J.G. Lockwood, 1975: Reply to commentary about the above article. Quart. J. Roy. Met. Soc., 101, 390-392.

De Bruin, H.A.R. and A.A.M. Holtslag, 1982: A simple parametrization of the surface fluxes of sensible and latent heat during daytime compared with the Penman-Monteith concept. J. Appl. Meteor., 21, 000-000 (accepted for publication).

Davies, J.A. and T.C. Uboegbulam, 1979: Parameterizations of surface incoming radiation in tropical cloudy conditions. Atmosphere-Ocean, 17, 14-23.

Deheer-Amissah, A., U. Högström and A.S. Smedman-Högström, 1981: Calculation of sensible and latent heat fluxes and surface resistance from profile data. Boundary Layer Meteorol., 20, 35-49.

Driedonks, A.G.M., H. van Dop and W.H. Kohsiek, 1978: Meteorological observations of the 213 m mast at Cabauw in the Netherlands. Proceedings of the fourth Symposium on Meteorological Observations and Instrumentation, A.M.S., Boston, Mass., 41-46.

Dyer, A.J., 1974: A review of flux-profile relationships. Boundary-Layer Meteorol., 7, 363-372.

Garratt, J.R. and B.B. Hicks, 1973: Momentum, heat and water vapour transfer to and from natural and artificial surfaces. Quart. J. R. Met. Soc., 99, 680-687.

Gay, L.W., 1971: The regression of net radiation upon solar radiation. Arch. Met. Geoph. Biokl., Ser. B, 19, 1-14.

Hicks, B.B., 1981: An examination of turbulence statistics in the surface boundary layer. Bound.-Layer Meteor., 21, 389-402.

Kasten, F. and G. Czeplak, 1980: Solar and Terrestrial radiation dependent on the amount and type of cloud. Solar Energy, 24, 177-189.

Lind, R.J. and K.B. Katsaros, 1982: A model of Longwave Irradiance for use with surface observations. J. Appl. Meteor., 21, 1015-1023.

Lumb, F.E., 1964: The influence of cloud on hourly amounts of total solar radiation at the sea surface. J. Roy. Met. Soc., 90, 43-56.

Monteith, J.L., 1981: Evaporation and surface temperature. Quart. J. Roy. Met. Soc., 107, 1-27.

Monteith, J.L. and G. Szeicz, 1961: The radiation balance of bare soil and vegetation. Quart. J. Roy. Met. Soc., 87, 159-170.

Nielsen, L.B., L.P. Prahm, R. Berkowicz and K. Conradsen, 1981: Net incoming radiation estimated from hourly global radiation and/or cloud observations. J. of Clim., 1, 255-272.

Nieuwstadt, F.T.M., 1978: The computation of the friction velocity u_* and the temperature scale T_* from temperature and wind velocity profiles by least-square methods. Boundary-Layer Meteorol., 14, 235-246.

Oke, T.R., 1978: Boundary Layer Climates. Methuen, London, 372 pp.

Pasquill, F., 1974: Atmospheric Diffusion. Wiley, Chichester, 429 pp.

Paulson, C.A., 1970: The mathematical representation of wind speed and temperature profiles in the unstable atmospheric surface layer. J. Appl. Meteor., 9, 856-861.

Paltridge, G.W. and C.M.R. Platt, 1976: Radiative processes in meteorology and climatology. Development in Atm. Science, 5, Elsevier, Amsterdam, 318 pp.

Reiff, J., A.P. van Ulden, G. Cats, D. Blaauboer and H.A.R. de Bruin, 1982: An air-mass transformation model for short range weather forecasting. Submitted to Mon Wea. Rev.

Sellers, W.D., 1965: Physical Climatology, University of Chicago press, Chicago, 272 pp.

Smith, F.B. and R.M. Blackall, 1979: The application of field experiment data to the parameterization of the dispersion of plumes from ground level and elevated sources. In Mathematical Modelling of Turbulent Diffusion in the Environment. J. Harris, ed., London, Academic Press, 500 pp.

Swinbank, W.C., 1963: Longwave radiation from clear skies. Quart. J. Roy. Met. Soc., 89, 339-348.

Thom, A.S. and H.R. Oliver, 1977: On Penman's equation for estimating regional evaporation. Quart. J. R. Met. Soc., 103, 345-357.

Van Dop, H., B.J. de Haan and C.A. Engeldal, 1982: The KNMI mesoscale air pollution transport model. Scientific Report W.R. 82-6, KNMI, De Bilt, 76 pp.

Wieringa, J., 1976: An objective exposure correction method for average wind speeds measured at a sheltered location. Quart. J. Roy. Met. Soc., 102, 241-253.

Wieringa, J., 1980: Representativeness of wind observations at airports. Bull. Am. Meteor. Soc., 61, 962-971.

Wieringa, J., 1983: Description requirements for assessment of non-ideal wind stations -- for example Aachen. J. Wind Engin. Industr. Aerodyn., 11, 111-121.

Table 1

Summary of the methods in this paper which are used to obtain the output of the scheme with the necessary input data.

Section	Parameterized quantity	Method	Input data
2	Incoming solar radiation (K^+)	Parameterization of the transmissivity of the atmosphere	Solar elevation (ϕ; see appendix B) Total cloud cover (N) Turbidity coefficients (a_1, a_2) Cloudiness coefficients (b_1, b_2)
3	Net radiation(Q^*)	Parameterization of the terms in the surface radiation budget	Incoming solar radiation (K^+) Air temperature (T) Longwave radiation coefficient (c_1) Total cloud cover (N) Cloudiness coefficient (c_2) Surface Albedo (r) Surface heating coefficient (c_3)
4	Sensible heat flux (H) Latent heat flux (λE)	Parameterization of the terms in the surface energy budget	Net radiation (Q^*) Air temperature (T) Surface moisture parameters (α and β)
5	Friction velocity (u_*) Obukhov stability parameter (L)	Monin-Obukhov similarity theory	Sensible heat flux (H) Wind speed (U_z) Surface roughness length (z_o)

Table 2

Comparison of the turbidity coefficients a_1 and a_2 of Eq. (1) for several locations.

$a_1(Wm^{-2})$	$a_2(Wm^{-2})$	Location	Reference
910	-30	Hamburg ($53^{o}38'N$, $9^{o}50'E$)	Kasten and Czeplak (1980)
990	-30	Harrogate ($54^{o}N$, $1^{o}30'W$)	Collier and Lockwood (1975)
1100	-50	North Atlantic ($52^{o}30'N$, $20^{o}W$)	Lumb (1964), obtained from his Fig. 1a
1098	-65	Boston ($42^{o}13'N$, $71^{o}7'W$)	Haurwitz (1945) obtained after expansion of his equation $K_o^+ = 1098 \sin\phi \exp(-0.059/\sin\phi)$
1041	-69	De Bilt ($52^{o}06'N$, $5^{o}11'E$)	This study (correlation coefficient r = 0.98, root mean square error σ = 40 Wm^{-2}, which is 9.5% of the observed average)

Table 3a

Comparison of hourly values of observed incoming solar radiation K^+ with calculated values of (1) and (2) for De Bilt in three classes of total cloud cover N and for the whole data set. The data cover one year of measurements for solar elevation $\phi > 10$ degrees. The calculations were done with $a_1 = 990\ Wm^{-2}$, $a_2 = -30\ Wm^{-2}$, $b_1 = -0.75$ and $b_2 = 3.4$.

	$N \leq 0.25$	$0.25 < N < 0.75$	$N \geq 0.75$	all N
n	504	564	1944	3012
$\bar{x}$	438.3	430.4	232.9	304.2
$\bar{y}$	422.9	388.4	231.3	292.8
r	0.980	0.908	0.820	0.906
σ	46.7	91.9	86.3	82.2
$\sigma/\bar{y}$	0.110	0.237	0.373	0.281

Notes:

n : number of measurements

x : calculated value

y : observed value

$\bar{x}$, $\bar{y}$: averages of x, y respectively

σ : root mean square error $\{\overline{(y-x)^2}\}^{\frac{1}{2}}$

r : correlation coefficient

Table 3b

As table 3a, but here the comparison is made for 30-minute averages at Cabauw. Because there were no cloud observations available at Cabauw, we took the average of observations at four weather stations around Cabauw (within 40 km). See notes of table 3a.

	$N \leq 0.25$	$0.25 < N < 0.75$	$N \geq 0.75$	all N
n	252	568	923	1743
$\overline{x}$	470.9	421.8	231.4	328.1
$\overline{y}$	430.5	363.1	214.0	293.9
r	0.983	0.889	0.819	0.904
σ	54.8	105.1	88.3	90.3
$\sigma/\overline{y}$	0.130	0.289	0.413	0.307

Table 4a

Comparison of the observed net radiation Q^* at Cabauw with calculated values using Eq. (11) and measured values of K^+ in unstable conditions. Here N is total cloud cover. See notes of table 3a.

	$N \leq 0.25$	$0.25 < N < 0.75$	$N \geq 0.75$	all N
n	168	384	447	999
$\overline{x}$	271.3	241.7	181.8	219.9
$\overline{y}$	286.7	246.7	191.7	228.8
r	0.990	0.983	0.973	0.982
σ	28.4	24.3	23.7	24.8
$\sigma/\overline{y}$	0.099	0.099	0.124	0.086

Table 4b

As table 4a, but here the calculated values are obtained from Eq. (11) and calculated values of K^+ using Eqs. (1) and (2).

	$N \leq 0.25$	$0.25 < N < 0.75$	$N \geq 0.75$	all N
n	168	384	447	999
$\bar{x}$	298.0	276.5	179.4	236.7
$\bar{y}$	286.7	246.7	197.7	228.8
r	0.973	0.870	0.714	0.857
σ	36.3	67.8	66.9	63.2
$\sigma/\bar{y}$	0.127	0.275	0.349	0.219

Table 5

The dependence of the ratios γ/s and $(\gamma/s)/(1 + \gamma/s)$ on temperature (see Eq. (11)) for standard pressure P = 1000 mb.

T (°C)	γ/s	$\frac{\gamma/s}{1 + \gamma/s}$
-5	2.01	0.67
0	1.44	0.59
5	1.06	0.51
10	0.79	0.44
15	0.60	0.38
20	0.45	0.31
25	0.35	0.26
30	0.27	0.21
35	0.21	0.17

Table 6a

Comparison of the observed sensible heat flux H from profiles, using the calculated values of Eqs. (11), (13), (14) and measured values of K^+ in unstable conditions. Here N is total cloud cover. See notes of table 3a.

	$N \leq 0.25$	$0.25 < N < 0.75$	$N \geq 0.75$	all N
n	168	384	447	999
$\overline{x}$	67.7	60.4	42.9	53.8
$\overline{y}$	63.2	61.3	46.2	54.9
r	0.795	0.788	0.803	0.800
σ	27.3	29.1	22.3	26.0
$\sigma/\overline{y}$	0.432	0.475	0.483	0.474

Table 6b

As table 6a, but here the calculated values are obtained with Eqs. (11), (13, (14) and calculated values of K^+ with Eqs. (1) and (2). See notes of table 3a.

	$N \leq 0.25$	$0.25 < N < 0.75$	$N \geq 0.75$	all N
n	168	384	447	999
$\overline{x}$	76.0	71.9	41.5	59.0
$\overline{y}$	63.2	61.3	46.2	54.9
r	0.785	0.652	0.524	0.640
σ	30.3	37.2	32.1	33.9
$\sigma/\overline{y}$	0.479	0.607	0.695	0.617

Table 7

Terrain classification by Wieringa (1980) in terms of aerodynamical roughness length z_o.

Class	Short terrain description	z_o (m)
1	Open sea, fetch at least 5 km	0.0002
2	Mud flats, snow; no vegetation, no obstacles	0.005
3	Open flat terrain; grass, few isolated obstacles	0.03
4	Low crops; occasional large obstacles, $x/h > 20$	0.10
5	High crops; scattered obstacles, $15 < x/h < 20$	0.25
6	Parkland, bushes; numerous obstacles, $x/h \sim 10$	0.5
7	Regular large obstacle coverage (suburb, forest)	(1.0)
8	City center with high- and low-rise buildings	?-?

Notes: Here x is a typical upwind obstacle distance and h the height of the corresponding major obstacles. Class 8 is theoretically intractable within the framework of boundary layer meteorology and can better be modeled in a wind tunnel. For simple modeling applications it may be sufficient to use only classes 1, 3, 5, 7 and perhaps 8.

Table 8

The dependence of the solar elevation in transition hours (ϕ_o) on total cloud cover (N). H_1 and H_2 are the fluxes of sensible heat obtained from profiles and calculated by way of the proposed scheme, respectively. See appendix C.

N	ϕ_o	$H_1(Wm^{-2})$	$H_2(Wm^{-2})$
0	13	-8	3
0.125	12	-4	1
0.25	12	-0	-1
0.375	12	-5	0
0.5	12	-7	4
0.625	13	-3	5
0.75	13	-3	1
0.875	15	-3	0
1	23	-2	-1

Figure captions

Fig. 1. Comparison of observed half-hourly averages of the incoming solar radiation (K^+_{obs}) with estimated values of (1) and (2) (K^+_{est}) at Cabauw.

Notes: In this figure a random selection is given of the whole data set. Squares refer to clear skies ($N \leq 0.25$) and triangles refer to other conditions. Units are in Wm^{-2}; r and σ are the correlation coefficient and the root mean square error of the whole data set, respectively.

Fig. 2. Comparison of the correction term $CT = 4\sigma T^3(T_s - T)$ of Eq. (7) with half-hourly observations of
a. the incoming solar radiation K^+
b. the net radiation Q^*
c. the sensible heat flux H
at a micrometeorological field in Cabauw for four summerdays in 1977. Units are Wm^{-2}.

Fig. 3. Comparison of measured half-hourly averages of the net radiation at Cabauw (Q^*_{obs}) with estimated values (Q^*_{est}) of (11) using measured incoming solar radiation. See notes of Fig. 1.

Fig. 4. As Fig. 3, but here Q^*_{est} is obtained with (11) and calculated values of K^+ using (1) and (2). See notes of Fig. 1.

Fig. 5. Comparison of the sensible heat flux obtained from profiles of wind and temperature (H_{obs}) with the sensible heat flux estimated with (11), (13) and (14) using measured incoming solar radiation (H_{est}). See notes of Fig. 1.

Fig. 6. As Fig. 5, but here H_{est} is obtained from (11), (13) and (14) with calculated values of K^+ using (1) and (2). See notes of Fig. 1.

Fig. 7. Comparison of the sensible heat flux obtained from measurements using Bowen's ratio method (H_{Bowen}) with the sensible heat flux obtained from wind and temperature profiles ($H_{profile}$) during the summer of 1977. See notes of Fig. 1.

Fig. 8. Comparison of the similarity ratio z_o/L obtained from profiles of wind and temperature (z_o/L_{obs}) with the estimated value from the proposed scheme (z_o/L_{est}). See notes of Fig. 1.

Figure 1

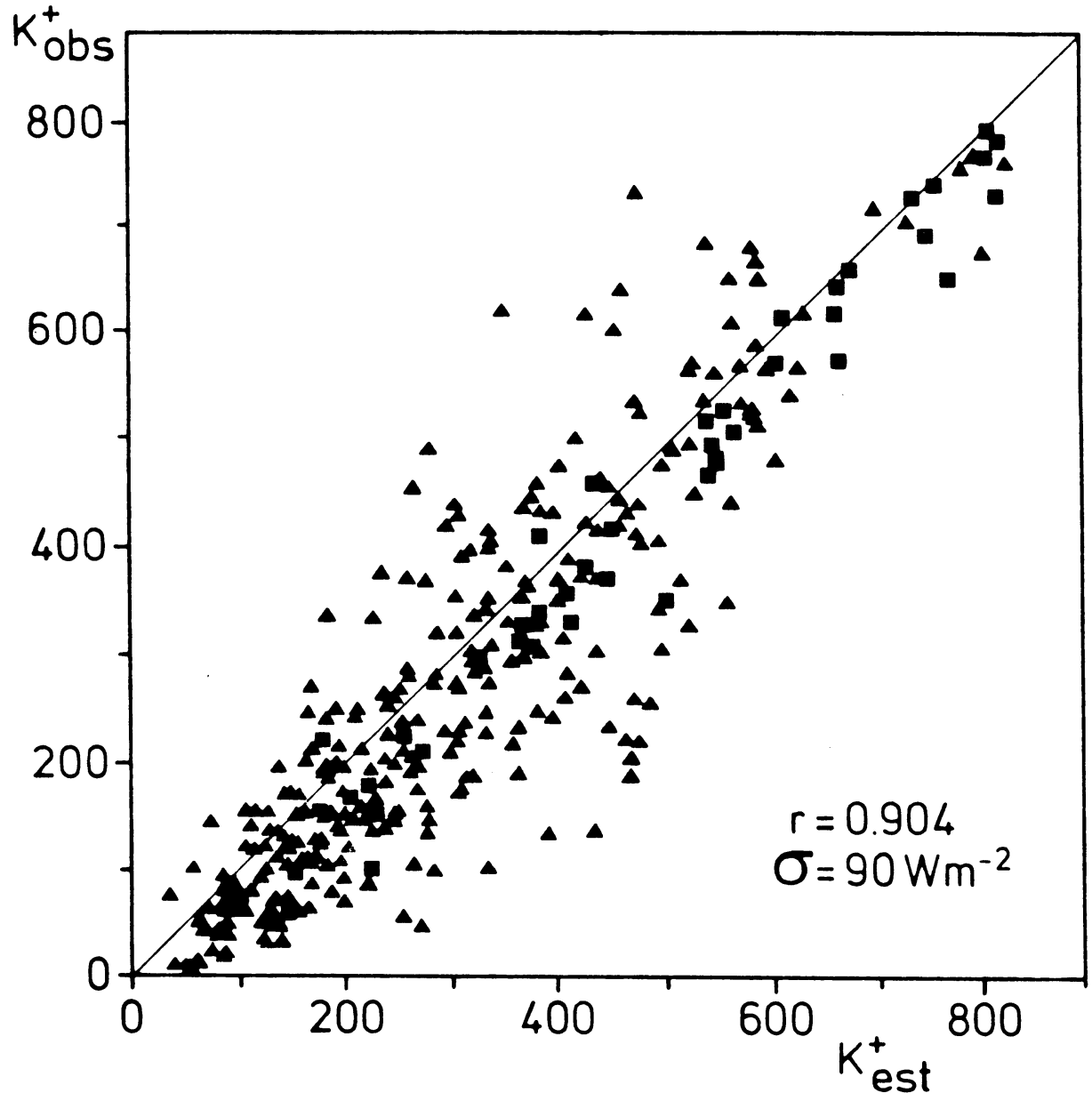

Figure 2

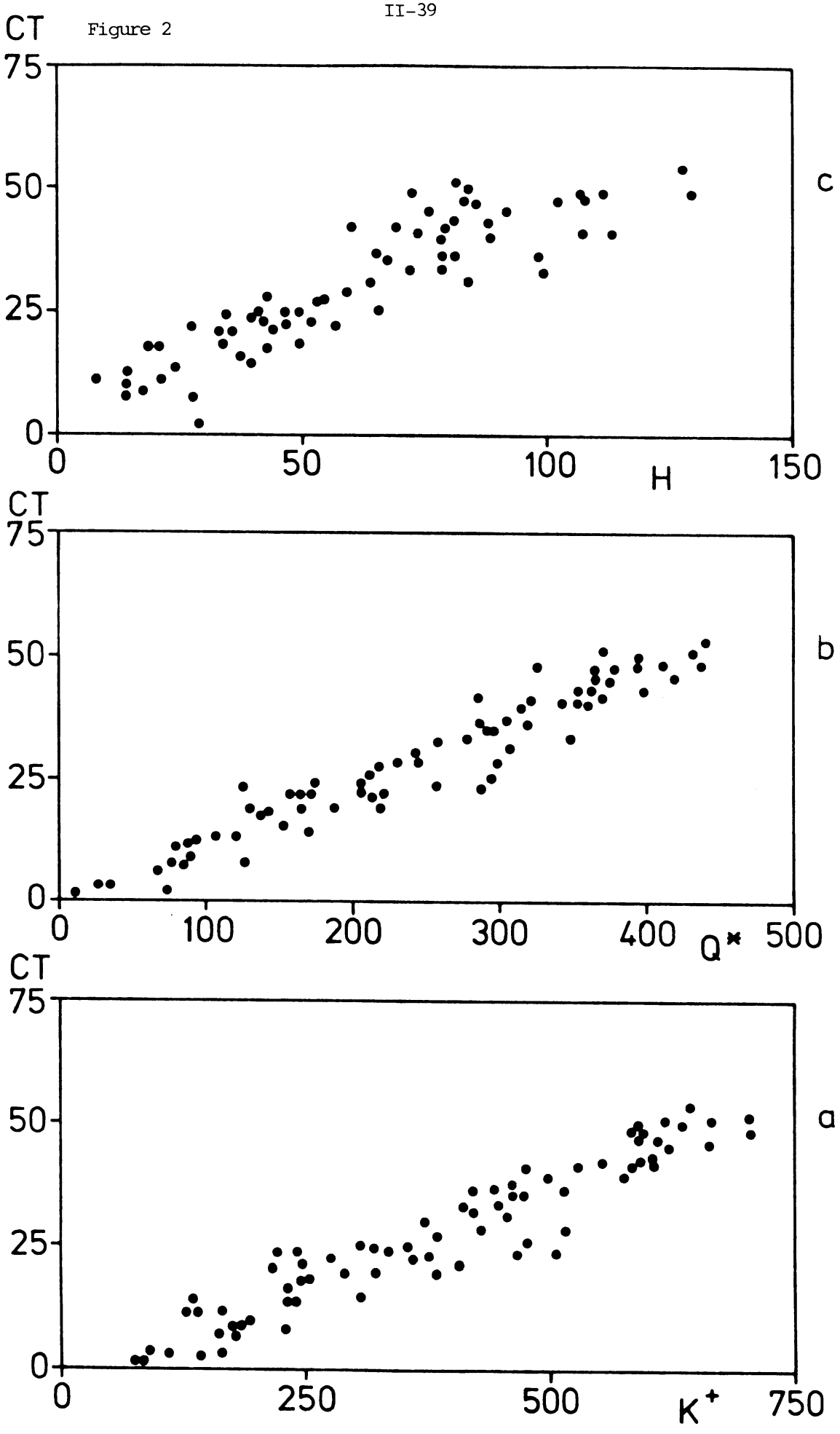
CT
75
50
25
0
0
50
100
150
H
c
CT
75
50
25
0
0
100
200
300
400
Q*
500
b
CT
75
50
25
0
0
250
500
K+
750
a

Figure 3

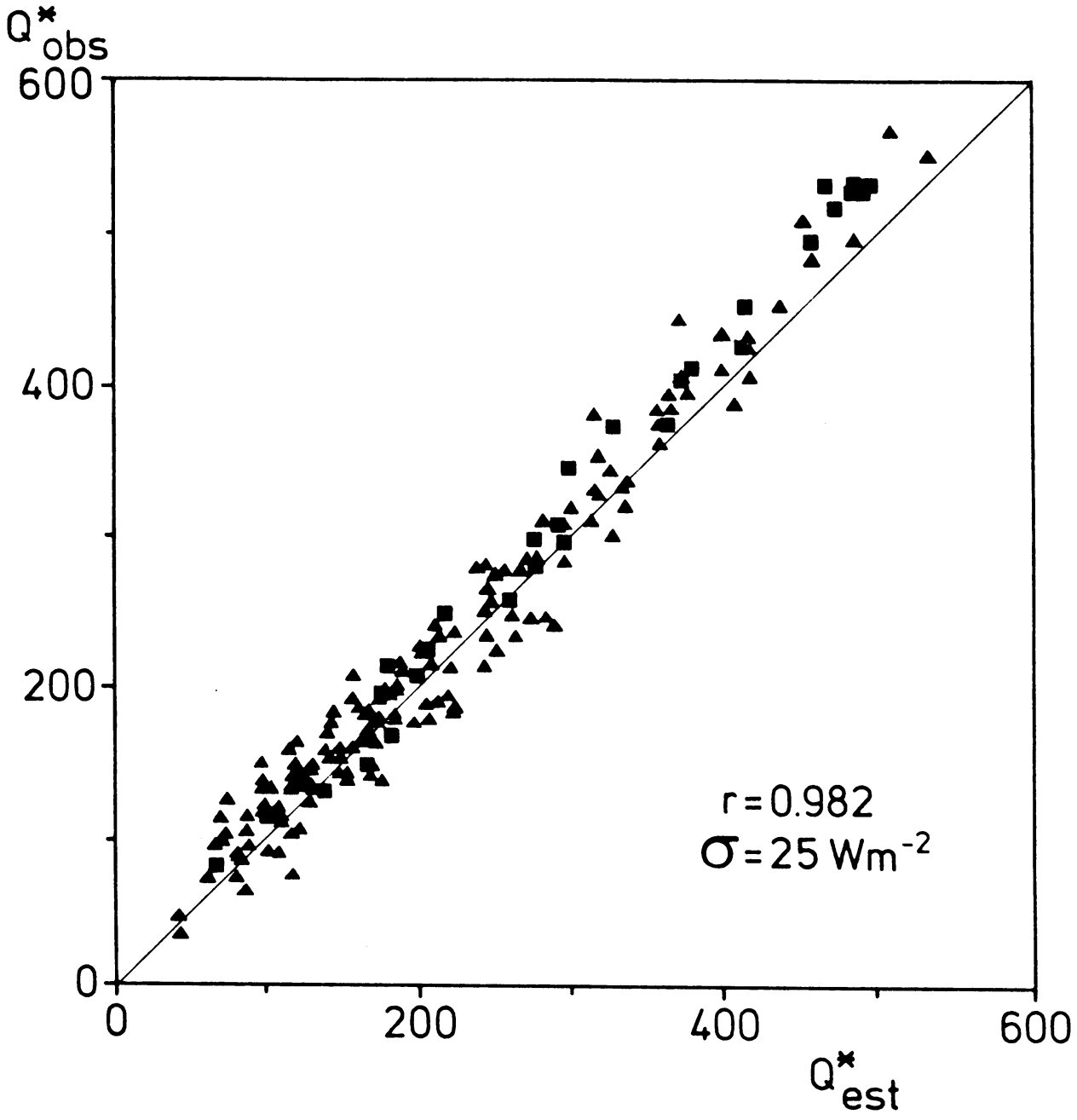

Figure 4

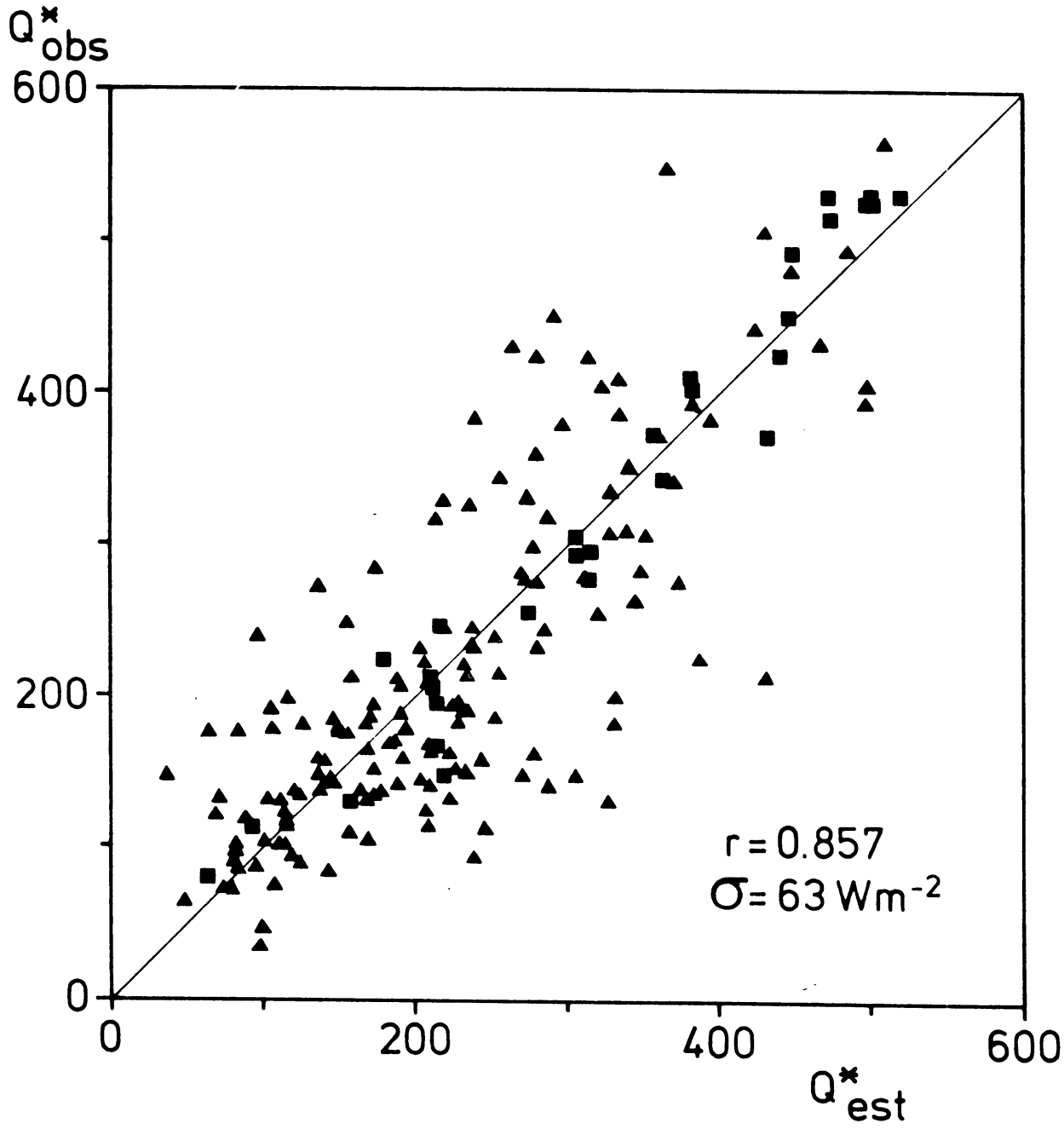

Figure 5

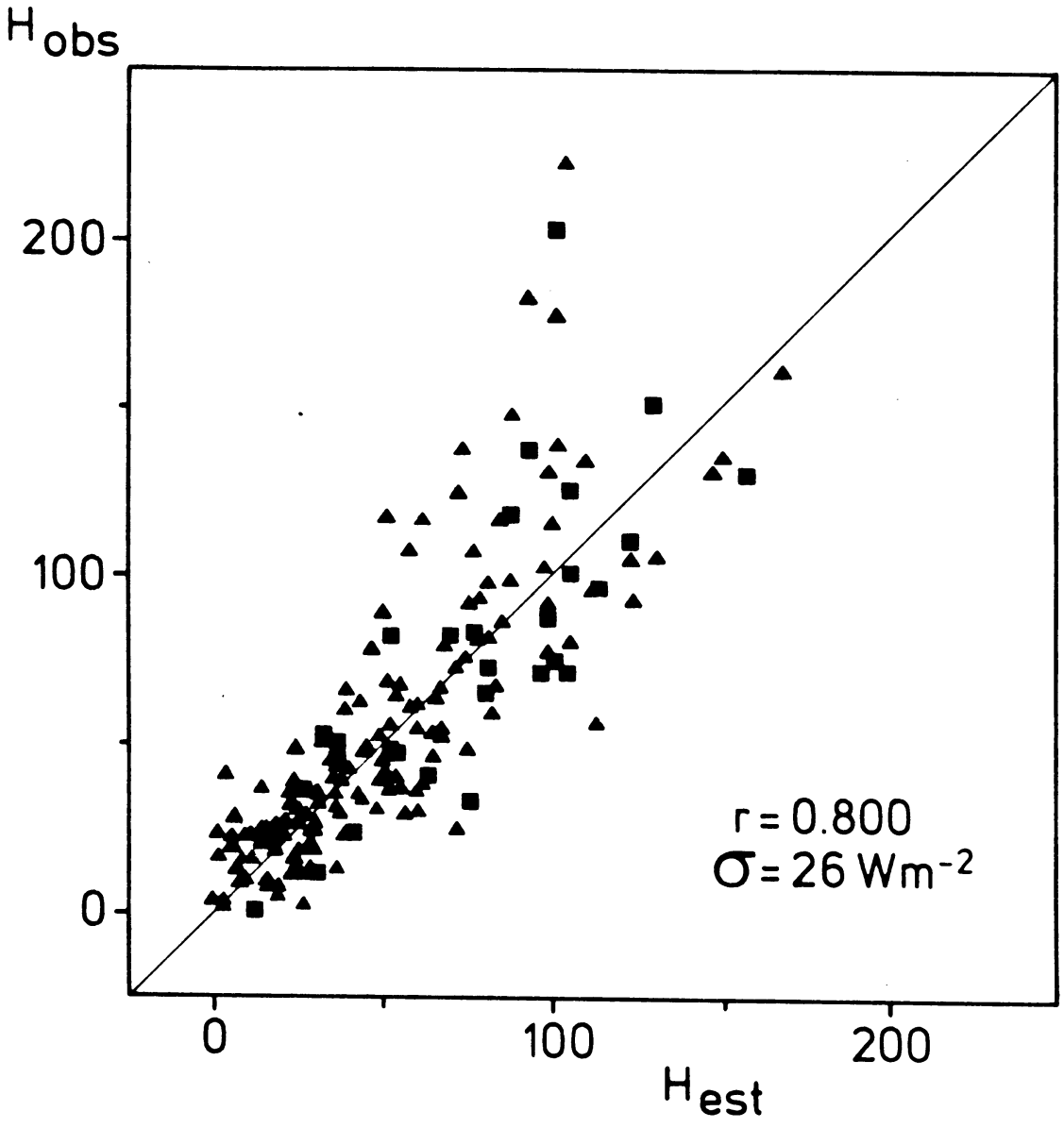

Figure 6

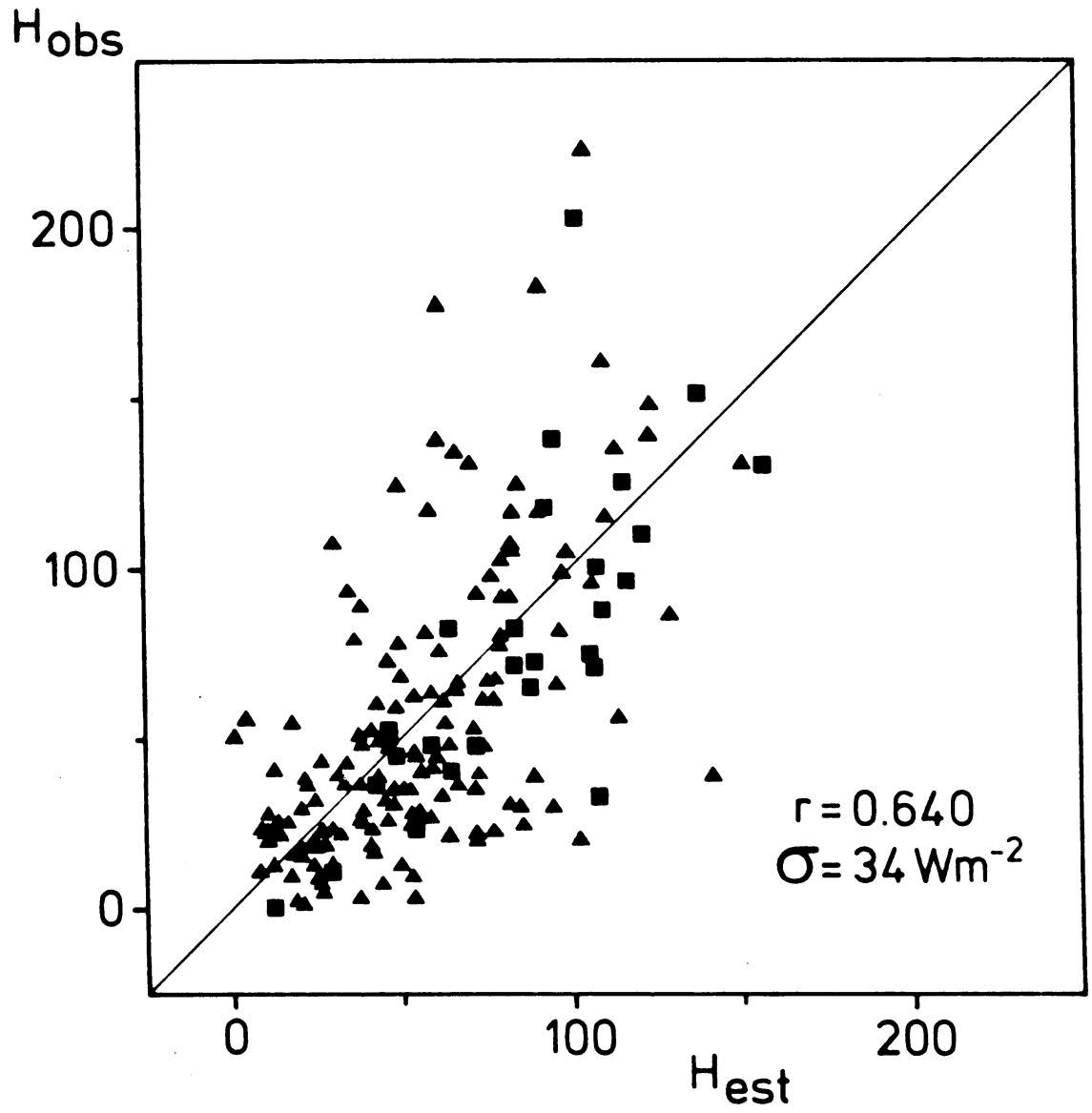

Figure 7

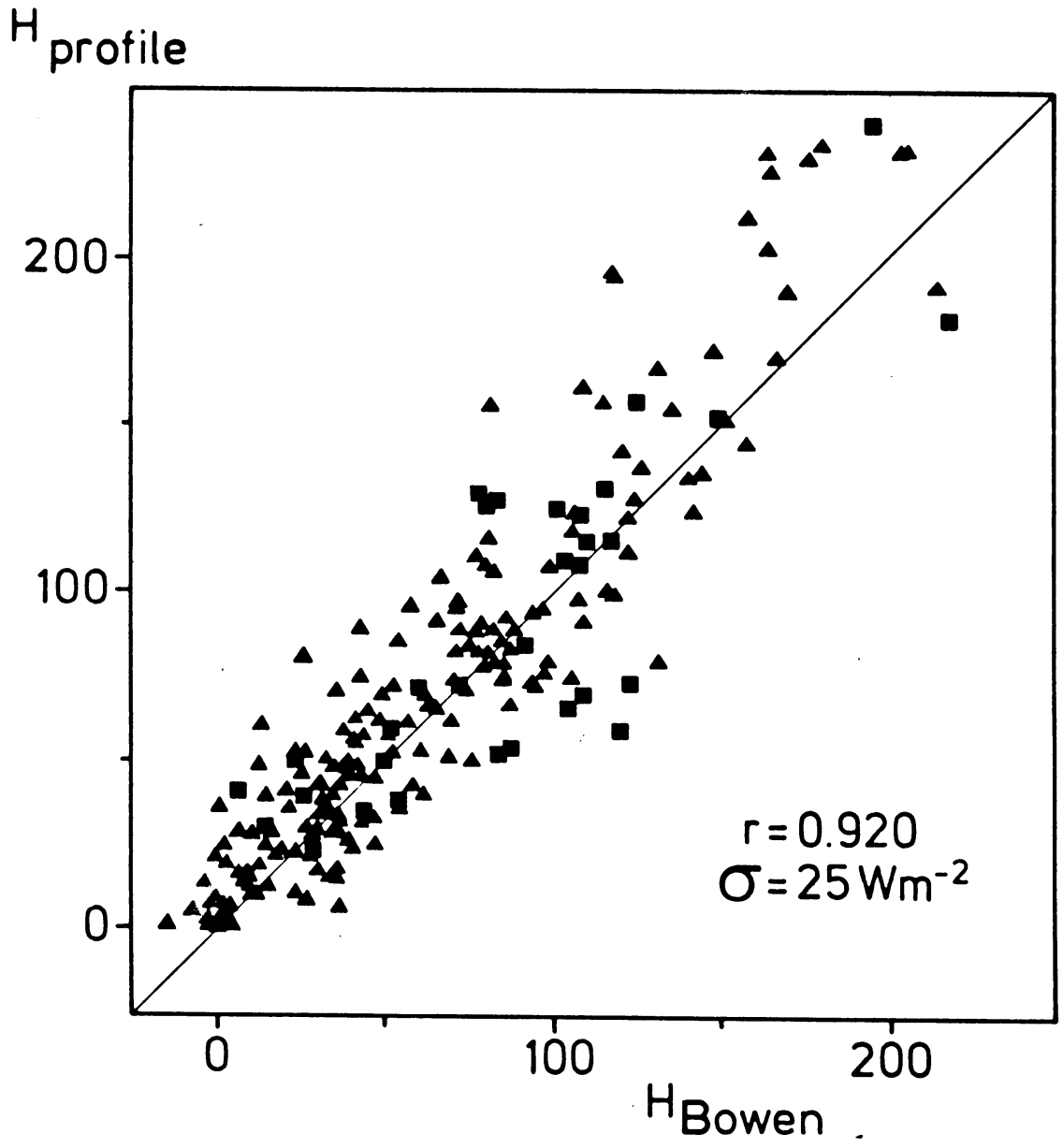

Figure 8

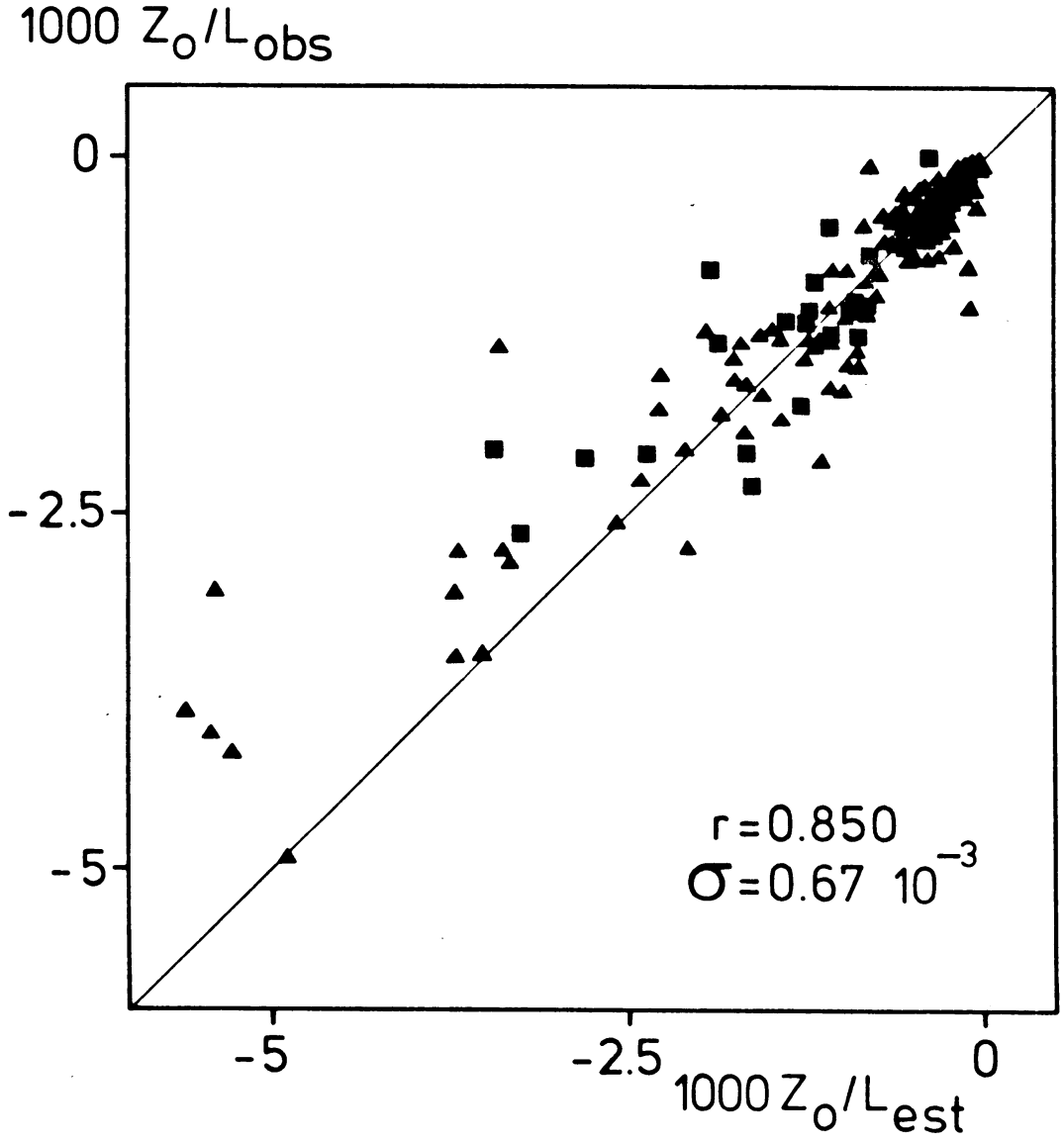

Hoofdstuk III

Simple estimates of nighttime surface fluxes from routine weather data.*

Abstract

This report deals with hourly estimates of the surface fluxes of heat and momentum from routine weather data during nighttime. For this purpose one year of measured profiles of wind and temperature are analysed. With the measured profiles the friction velocity (u_*) and the temperature scale (θ_*) are computed using the flux-profile relations of Dyer (1974). It appears that θ_* decreases for very high and low windspeeds. But in an intermediate region of u_* it follows that θ_* decreases mainly with increasing total cloud cover (N). These results are consistent with the analysis by Venkatram (1980), which is based on the Prairie Grass, Kansas and Minnesota data. The behaviour of θ_* with u_* and N is described. This implies that the surface fluxes can be obtained from a single windspeed, the surface roughness length, total cloud cover and the air temperature. The required procedures are fairly simple and are described in the paper. It is shown that the proposed scheme can furnish good estimates for the flux of sensible heat, the flux of momentum in terms of the friction velocity and the Obukhov stability parameter. With the scheme a satisfactory description can be given of the nocturnal surface layer.

1. Introduction.

The surface fluxes of heat and momentum are important parameters in the description of the atmospheric boundary layer. The fluxes determine the turbulent state and the stability of the surface layer. The fluxes are used in boundary layer models, air pollution models and for the description of profiles near the ground of wind and temperature.

In principle the fluxes can be measured. However, such measurements are difficult and in practice usually only standard meteorological data are available. So there is a need to relate the fluxes to routine weather data. It

* Referentie [6] van hoofdstuk I (zie ook referentie [24] van hoofdstuk I).

is the aim of this paper to establish such relations in stable conditions. For unstable conditions such relations are given by Holtslag and Van Ulden (1982), based on a parameterization of the surface energy budget.

The surface energy budget relates the flux of sensible heat H to the net radiation Q^*, the soil heat flux G and the flux of latent heat λE. It reads (Sellers, 1965):

$$H + \lambda E + G = Q^* \quad . \tag{1}$$

During nighttime Q^* is negative and it is mainly fed by H and G, because in the night evaporation is usually small for a vegetated surface. The soil heat flux G is a large fraction of Q^* and it is depending on the solar heating of the surface in the preceding day. Further Q^* is affected by windspeed and cloud cover (Holtslag and Van Ulden, 1980; Nielsen et al., 1981). In the following it is shown that also H is affected by windspeed. So modelling of the surface energy budget during nighttime is rather complicated.

Instead of trying to model H with the aid of the surface energy budget we may consider the temperature scale θ_* and the friction velocity u_*. These quantities are related to H by

$$H = -\rho\, c_p\, u_*\, \theta_* \quad , \tag{2}$$

where ρ is the density of air and c_p is the specific heat of air at constant pressure. The friction velocity is related to the flux of momentum τ by:

$$\tau = \rho\, u_*^2 \quad . \tag{3}$$

The friction velocity u_* and the temperature scale θ_* can be obtained from observed temperature and wind profiles (see section 2). However, normally the required data is not available and u_* and θ_* have to be obtained in an other way.

In this report θ_* is related to cloud cover and u_* (section 3). Consequently from θ_*, a surface roughness length and a single windspeed the friction velocity u_* is determined (section 4). Then the Obukhov stability parameter L, defined by

$$L = \frac{u_*^2}{k \frac{g}{T} \theta_*} \tag{4}$$

can be calculated. In (4) k is the Von Kármán constant, g the accelaration of gravity and T the air temperature. The quantities of the scheme will be compared with the "observed" quantities of wind and temperature profiles (section 2).

2. Observation of the fluxes

The surface fluxes of heat and momentum can be obtained from the profiles of temperature and wind applying Monin-Obukhov similarity theory.
The semi-empirical flux-profile relations of Dyer and Webb (see Dyer, 1974) read in their integral form:

$$u_* = k\, u_z \left[\ln\left(\frac{z}{z_o}\right) + \beta \frac{z}{L}\right]^{-1} , \qquad (5)$$

and

$$\theta_* = k\, \Delta\theta \left[\ln\left(\frac{z_2}{z_1}\right) + \frac{\beta(z_2-z_1)}{L}\right]^{-1} . \qquad (6)$$

Here L is given by (4), z_o is the surface roughness length, U_z the windspeed at a height z and $\Delta\theta$ is a temperature difference between the two heights z_2 and z_1. Further k is the von Kármán constant (k = 0.41) and β is an empirical contant (β = 5.2).

Using (4), (5) and (6) we can obtain u_*, θ_* and L from a single wind speed U_z, a temperature difference $\Delta\theta$, the air temperature T and the surface roughness length z_o. We use the following procedure. The surface roughness length is obtained from a method by Wieringa (1976, 1980), using routine wind measurements. Table 1 gives a crude estimate of z_o for eight classes of surface roughness lengths.

The calculation starts with L = 5 in (5) and (6). Then u_* and θ_* are obtained and L is calculated with (4). With this value for L the calculation of u_* and θ_* is repeated until successive values of L are within 1 percent. It follows that usually not more than 3 iterations are needed to achieve the required accuracy in L. Finally the surface fluxes H and τ are obtained with (2) and (3).

From one year of data at Cabauw (1 March 1977 - 1 March 1978) we have

used 30 minute averages of the observed temperature difference between z_2 = 10 m and z_1 = 0.6 m, the air temperature at screenheight (2 m) and the 10 m windspeed. Only hours are taken into account with no rain or fog and with 10 m windspeed $U_{10} > 1$ ms^{-1}. The results of this calculation are in agreement with the method of Nieuwstadt (1978), except in very stable conditions.

With Nieuwstadt's method u_* and θ_* are obtained applying least square techniques with weight factors to the observed wind and temperature profiles. We prefer to use the above method because the fluxes of Nieuwstadt's method are rather sensitive for the weight factors in very stable conditions. This problem does not occur in the above method. Besides of this the above method is less time consuming and it is more easy to handle.

3. Modelling of the temperature scale θ_*.

During stable conditions in the atmospheric surface layer the sensible heat flux H is negative and the turbulent temperature scale θ_* is positive (see (2)). In section 2 we have seen that a temperature difference $\Delta\theta$ is needed to obtain θ_*. However, normally $\Delta\theta$ is not available and θ_* must be obtained in an other way.

Venkatram (1980) suggests that θ_* is nearly constant in stable conditions. According to data of the Prairie Grass, Kansas and Minnesota experiments

$$\theta_* = 0.08 \text{ (K)} \; . \qquad (7)$$

This estimate is based mainly on observations made during clear nights in homogeneous conditions. We will extend (7) to cloudy conditions and we will investigate a possible dependence of θ_* on the friction velocity u_*.

Fig. 1 shows a plot of θ_* versus u_* for two classes of total cloud cover (N) during nighttime. Each point is an average of at least 15 observations of θ_* . In the figure lines are drawed for which the Obukhov stability parameter L = 10 m and the sensible heat flux H = -60 Wm^{-2}.

In Fig. 1 it is seen that between the two lines θ_* is almost independent from u_* but clearly a function of cloud cover.
From our data we found that:

$$\theta_* = 0.09\ (1 - 0.5\ N^2)\ , \qquad (8)$$

yields satisfactory estimates of θ_* (in K) for $L > 10$ m and $H < -60\ Wm^{-2}$. For 1643 (30 minute) averages of θ_* we found a root mean square error $\sigma = 0.026$ K and a correlation coefficient $r = 0.5$ between (8) and θ_* observed from profiles (section 2). The total cloud cover was interpolated from four synoptic stations around Cabauw (within 40 km). The estimate of (8) is consistent with (7), because (7) is based mainly on measurements made in clear nights.

For very stable conditions ($L < 10$) we see from Fig. 1 that θ_* decreases with u_*. A simple empirical solution to obtain the fluxes in these conditions is dicussed in section 4. At extremely high windspeed we obtain with (2) and (8) that the sensible heat flux increases indefinitely. We may expect that in these cases the surface radiation budget puts a limit on H. From our data it follows that $H = -60\ Wm^{-2}$ is an appropriate limit for H (see Fig. 1).

Our estimate (8) applies when the sun is below the horizon. When the sun is above the horizon the atmosphere becomes less stable until at a certain solar elevation ϕ_o the atmosphere becomes unstable. The latter occurs for $\phi_o \simeq 13$ degrees for $N \leq 0.75$ up to $\phi_o = 23$ degrees for $N = 1$ (Holtslag and Van Ulden, 1982).

When the heat flux is negative and the sun above the horizon the solar elevation ϕ enters the scheme for θ_*. We propose:

$$\theta_*^t = \theta_*^n \left\{1 - \left(\frac{\phi}{\phi_o}\right)^2\right\} \qquad (9)$$

$$\text{for } 0 \leq \phi \leq \phi_o\ .$$

Here θ_*^n is the estimate of (8), θ_*^t is the estimate in transition hours and ϕ_o is the solar elevation for which a zero heat flux occurs. The latter quantity can be obtained from the daytime scheme of Holtslag and Van Ulden (1982). Here also a scheme is given for ϕ which uses geographical position and time. It appears that the estimate of (9) provides a comparable fit to data for transition hours as (8) does for night data.

4. Estimation of the fluxes from a modelled θ_*.

In this section we will derive the friction velocity u_* with our estimates for the temperature scale θ_* of the preceding section. Then the fluxes and the Obukhov stability parameter are obtained with (2), (3) and (4).

We may substitute (4) into (5) to obtain a quadratic equation in u_* for a given θ_*, U_z, z_o and T. The solution for u_* reads:

$$u_* = \tfrac{1}{2} \{u_{*N} + D_{u_*}^{\frac{1}{2}}\} , \tag{10}$$

where D_{u_*} is given by:

$$D_{u_*} = u_{*N}^2 - \frac{4 \beta k g z \theta_*}{T \ln z/z_o} . \tag{11}$$

Further u_{*N} is the value of u_* without stability correction ($L = \infty$ in (5)) given by

$$u_{*N} = \frac{k U_z}{\ln z/z_o} . \tag{12}$$

The value of θ_* is given by (8) or (9) and z_o can be obtained from a method by Wieringa (1976, 1980) or table 1. Then it is seen that u_{*N}, D_{u_*} and thus u_* can be calculated with U_z and T, but we have to require that $D_{u_*} \geq 0$.

The requirement $D_{u_*} \geq 0$ may reduce the practical use of (10). Let us compute for z = 10 m the values for the friction velocity u_{*o} and the Obukhov stability parameter L_o which occur at $D_{u_*} = 0$. Then it follows with (4), (10) and (11):

$$u_{*o} = \tfrac{1}{2} u_{*N} \tag{13}$$

and

$$L_o = \frac{10 \beta}{\ln \frac{10}{z_o}} . \tag{14}$$

With $\beta = 5.2$ and $z_o = 0.15$ (average value at Cabauw) we obtain with (14) $L_o = 12.4$ m. Then the 10 m windspeed U_{10} is $U_{10} = 2.6$ ms^{-1} at clear skies and $U_{10} = 1.8$ ms^{-1} at total overcast. Here we have taken T = 280 K in (11). It follows

that $D_{u_*} < 0$ occurs at low windspeed and very stable conditions. These conditions correspond to the small values of θ_* and u_* in Fig. 1.

From Fig. 1 it is seen that for the very stable conditions ($L < 10$) u_* and θ_* both tend to zero. To obtain the fluxes in these conditions we propose a linear interpolation between $\theta_* = u_* = 0$ and θ_* estimated with (8) or (9) and u_* obtained with (13). Then it follows

$$\theta_* = 2\ \theta_{*s}\ \frac{u_*}{u_{*N}}\ , \qquad (15)$$

where θ_{*s} is the value of (8) or (9) and u_{*N} is given by (12). With (15) u_* and L can be obtained in the very stable conditions using (4), (5) and (12). It reads for u_*:

$$u_* = \frac{k\ U_{10}}{\ln \frac{10}{z_o}} - \frac{20\ \beta\ g\ \theta_{*s}}{T\ U_{10}}\ , \qquad (16)$$

where we have used the 10 m windspeed (U_{10}).
With (16) it follows that $u_* = 0$ for $U_{10} = 1.8$ ms^{-1} at clear skies decreasing to $U_{10} = 1.3$ ms^{-1} at total overcast. Beneath these small values of U_{10} the scheme gives $u_* = \theta_* = L = 0$.

With the above equations we can make estimates for θ_* and u_*. Then H, τ and L are given by (2), (3) and (4). We made a comparison of u_*, H and L of the scheme with corresponding values obtained from profiles (see section 2). We have used the 10 m windspeed, the air temperature at 2 m and total cloud cover interpolated from four synoptic stations around Cabauw (within 40 km). In 2 % of the cases H of the scheme $H < -60$ Wm^{-2}. Then we putted $H = -60$ Wm^{-2} and $u_* = u_{*N}$ given by (12). The latter estimate is within a few percent at these high windspeed cases. Results are shown in Figs. 2, 3 and 4 for nighttime hours. A distinction is made between cases with $D_{u_*} \geq 0$ and $D_{u_*} < 0$.

From the figures it is seen that rather good estimates for u_*, H and L can be obtained using our scheme. As expected the very stable cases show the largest deviations. However, on average of course the estimates of (15) and (16) are acceptable. These estimates are necessary in 10 % of the cases because then $D_{u_*} < 0$.

In the comparisons there is a bias because the same windspeed data has been used in the calculated and observed quantities. Nevertheless, our scheme will give reliable estimates for u_*, H and L in practice, because the fluxes

from profiles compare reasonable with those from turbulence measurements (Nieuwstadt, 1978).

5. Summary and conclusions

In this report a simple scheme is presented which relates the surface fluxes of heat and momentum to routine weather variables. The required input weather data are the air temperature at screenheight (2 m), the 10 m windspeed and the total cloud cover. Further the surface roughness length is needed. As such the scheme can serve as an alternative for the traditional Pasquill stability classification (Pasquill, 1974).

From one year of measured windspeed and temperature profiles it appears that the turbulent temperature scale (θ_*) can be described as a function of the friction velocity (u_*) and the total cloud cover (N). It follows that θ_* decreases with increasing cloud cover. Further it follows that θ_* also decreases for very high and low windspeeds. The results are consistent with the analysis by Venkatram (1980).

With the described relation between θ_*, u_* and N it is shown that the scheme provides good estimates for the friction velocity, the flux of sensible heat and the Obukhov stability parameter. Because of this and its simplicity we conclude that the scheme is useful for many applications in boundary layer meteorology.

At present the scheme is applied in the Dutch boundary-layer/trajectory model for short range weather forecasting (Reiff et al., 1982) and in the KNMI mesoscale air pollution transport model (Van Dop et al., 1982).

Acknowledgements.
The authors are grateful to Dr. A.C.M. Beljaars and Dr. A.G.M. Driedonks for comments on the draft of this report.

References

Dyer, A.J., 1974: A review of flux-profiles relationships. Boundary-Layer Meteorology, 7, 363-372.

Holtslag, A.A.M. and A.P. van Ulden, 1980: Estimates of incoming shortwave radiation and net radiation from standard meteorological data. Scientific Report, W.R. 80-6, K.N.M.I., De Bilt.

Holtslag, A.A.M. and A.P. van Ulden, 1982: A simple scheme for daytime estimates of the surface fluxes from routine weather data. Submitted to J. Appl. Meteor. (K.N.M.I. internal report FM-82-12).

Nielsen, L.B., L.P. Prahm, R. Berkowicz and K. Conradsen, 1981: Net incoming radiation estimated from hourly global radiation and/or cloud observations. J. of Clim., 1, 255-272.

Nieuwstadt, F.T.M., 1978: The computation of the friction velocity u_* and the temperature scale T_* from temperature and wind velocity profiles by least-square methods. Boundary-Layer Meteorol., 14, 235-246.

Pasquill, F., 1974: Atmospheric Diffusion. Wiley, Chichester.

Reiff, J., D. Blaauboer, H.A.R. de Bruin and A.P. van Ulden, 1982: A boundary-layer/trajectory model for short range weather forecasting. To be submitted to J. Appl. Meteor.

Sellers, W.D., 1965: Physical Climatology. University of Chicago Press, Chicago.

Van Dop, H., B.J. de Haan and C.A. Engeldal, 1982: The K.N.M.I. mesoscale air pollution transport model. To be submitted to Atm. Env.

Venkatram, A., 1980: Estimating the Monin-Obukhov length in the stable boundary layer for dispersion calculations. Boundary-Layer Meteorol., 19, 481-485.

Wieringa, J., 1976: An objective exposure correction method for average wind speeds measured at a sheltered location. Quart. J. R. Met. Soc., 102, 241-253.

Wieringa, J., 1980: Representativeness of wind observations at airports. Bull. Am. Meteor. Soc., 61, 962-971.

Table 1

Terrain classification by Wieringa (1980) in terms of aerodynamical roughness length z_o.

Class	Short terrain description	z_o (m)
1	Open sea, fetch at least 5 km	0.0002
2	Mud flats, snow; no vegetation, no obstacles	0.005
3	Open flat terrain; grass, few isolated obstacles	0.03
4	Low crops; occasional large obstacles, $x/h > 20$	0.10
5	High crops; scattered obstacles, $15 < x/h < 20$	0.25
6	Parkland, bushes; numerous obstacles, $x/h \sim 10$	0.5
7	Regular large obstacle coverage (suburb, forest)	(1.0)
8	City center with high- and low-rise buildings	?-?

Notes: Here x is typical upwind obstacle distance and h the height of the corresponding major obstacles. Class 8 is theoretically intractable within the framework of boundary layer meteorology and can better be modelled in a wind tunnel. For simple modelling applications it may be sufficient to use only classes 1, 3, 5, 7 and perhaps 8.

Figure captions

Fig. 1. The variation of the temperature scale θ_* (in K) with friction velocity u_* (in ms^{-1}) for clear skies (dots) and cloudy skies (triangles). In the figure N is total cloud cover, L is Obukhov stability parameter and H is the sensible heat flux.

Fig. 2. Comparison of 30 minute averages of the friction velocity u_* (in 0.01 ms^{-1}) obtained with profiles of wind and temperature with calculated values of the scheme. (σ = 0.03 ms^{-1}, r = 0.99).

Notes: In the figure a selection of the whole data set is given. Triangles refer to stable conditions with $D_{u_*} > 0$ and squares refer to conditions with $D_{u_*} < 0$ (see (11)). The root mean square error σ and the correlation coefficient r are calculated for the whole data set of 1643 hours during nighttime. The additions OBS and EST along the axes of the figure refer to observed from profiles and estimated with the present scheme, respectively.

Fig. 3. Comparison of observed and calculated 30 minute averages of the sensible heat flux H (in Wm^{-2}) (σ = 9.5 Wm^{-2}, r = 0.79). See notes of Fig. 2.

Fig. 4. Comparison of observed and calculated 30 minute averages of the Obukhov stability parameter L (in m) (σ = 50 m, r = 0.85). See notes of Fig. 2.

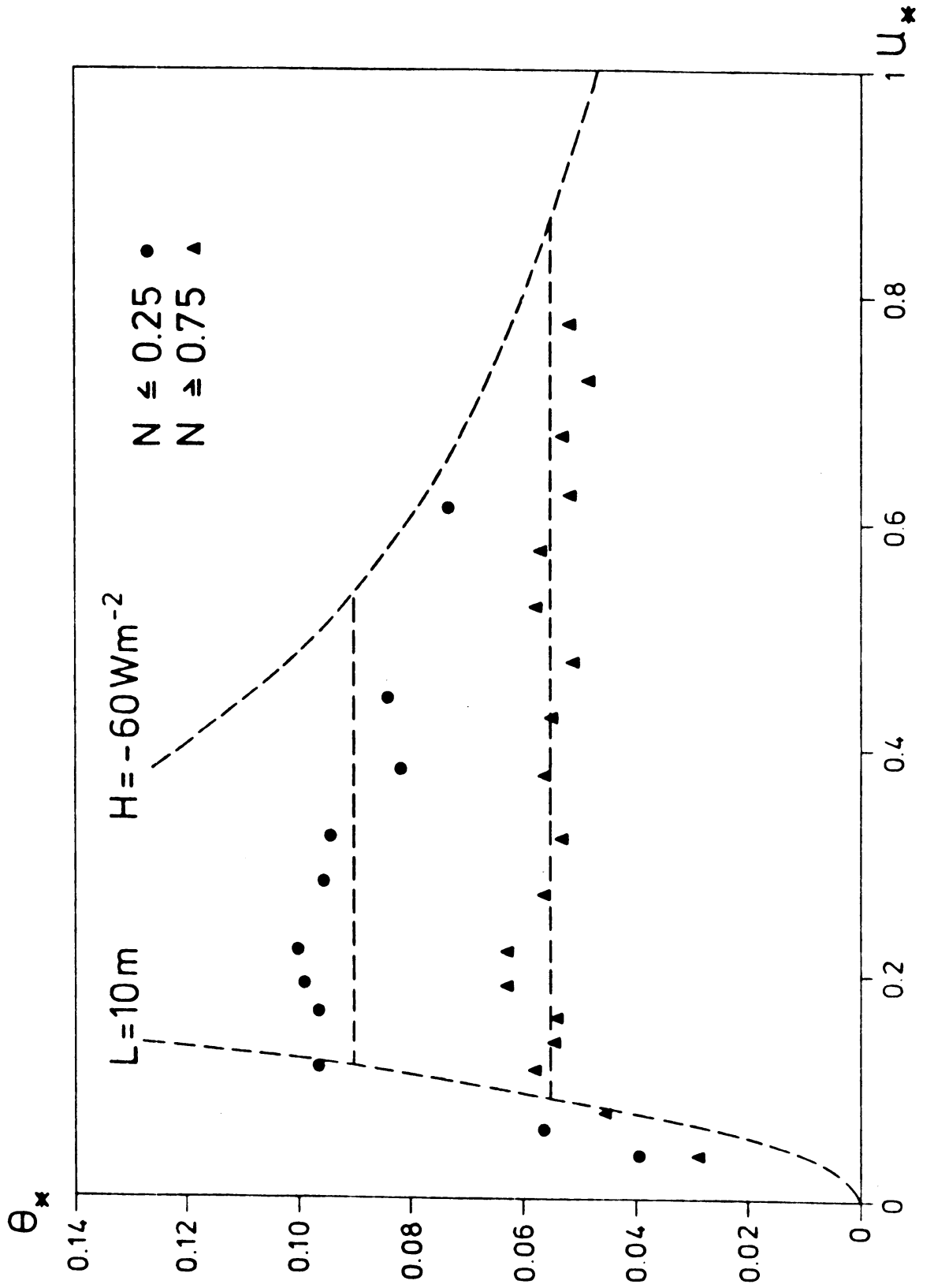
θ*
0.14
0.12
0.10
0.08
0.06
0.04
0.02
0
0
0.2
0.4
0.6
0.8
1
U*
L=10m
H=-60Wm-2
N ≤ 0.25 ●
N ≥ 0.75 ▲

Figure 1

Figure 2

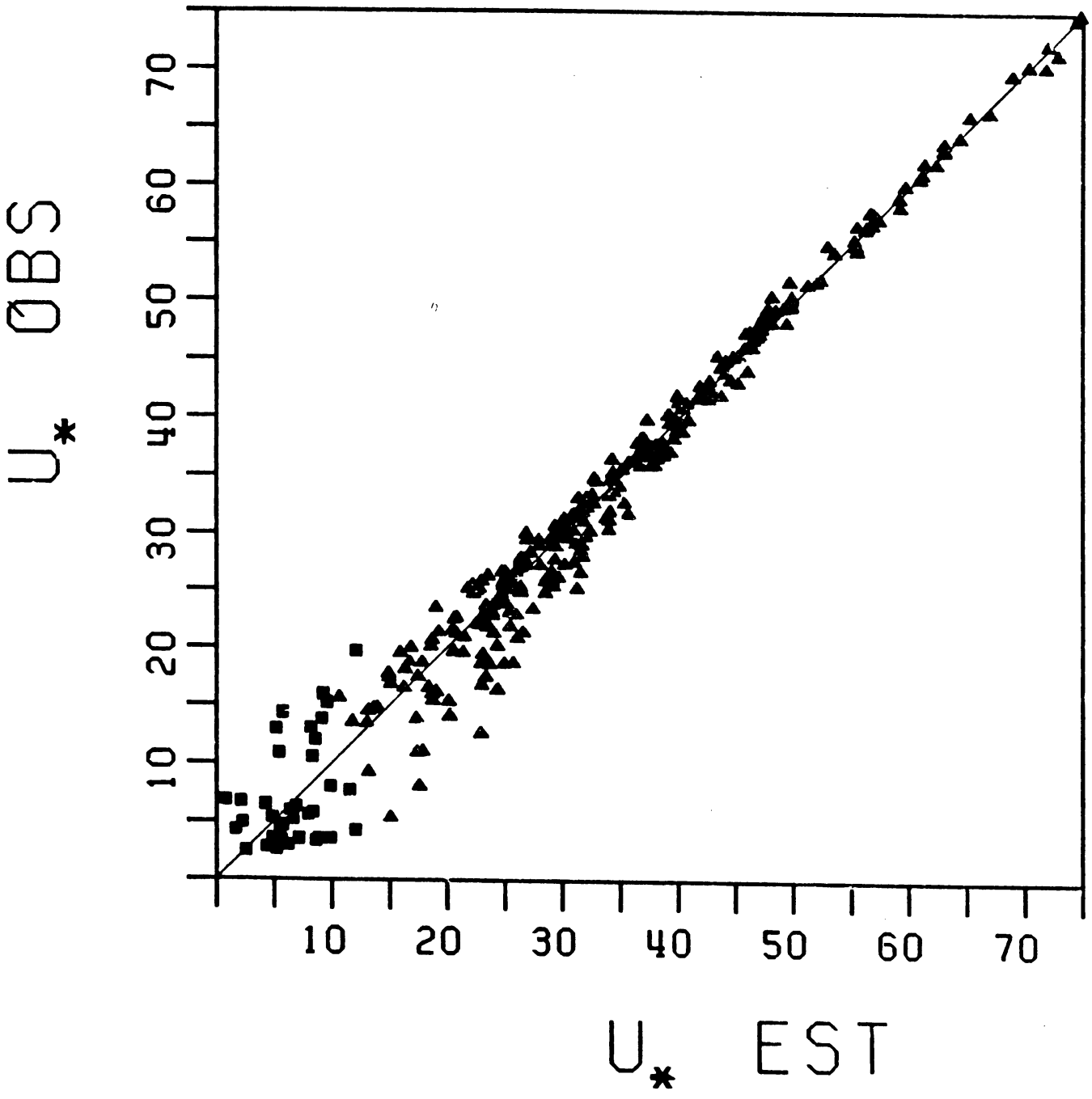

Figure 3

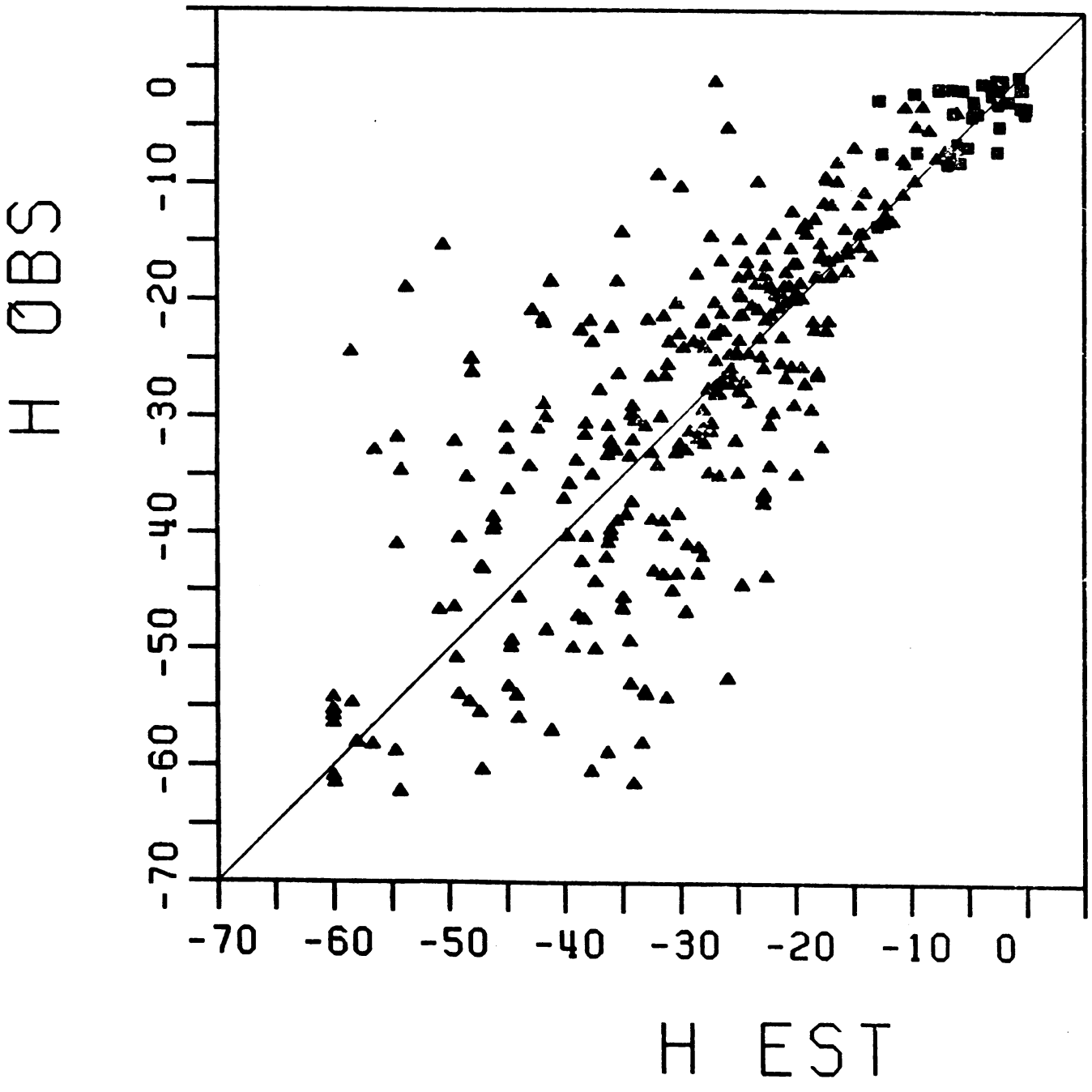

Figure 4